

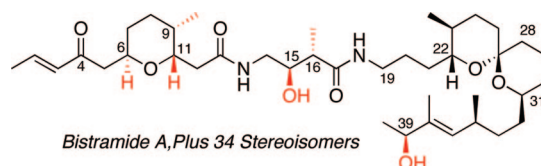
## Synthesis of a 35-Member Stereoisomer Library of Bistramide A: Evaluation of Effects on actin State, Cell Cycle and Tumor Cell Growth

Iwona E. Wrona,<sup>†</sup> Jason T. Lowe,<sup>†</sup> Thomas J. Turbyville,<sup>‡,§</sup> Tanya R. Johnson,<sup>‡</sup>  
Julien Beignet,<sup>†</sup> John A. Beutler,<sup>‡</sup> and James S. Panek<sup>\*,†</sup>

Department of Chemistry and Center for Chemical Methodology and Library Development (CMLD-BU), Boston University, 590 Commonwealth Avenue, Boston, Massachusetts 02215, and Molecular Targets Development Program, National Cancer Institute at Frederick, Building 560-15, Frederick, Maryland 21702

panek@bu.edu

Received October 24, 2008



Synthesis and preliminary biological evaluation of a 35-member library of bistramide A stereoisomers are reported. All eight stereoisomers of the C1–C13 tetrahydropyran fragment of the molecule were prepared utilizing crotylsilane reagents **9** and **10** in our [4+2]-annulation methodology. In addition, the four isomers of the C14–C18  $\gamma$ -amino acid unit were accessed via a Lewis acid mediated crotylation reaction with use of both enantiomers of organosilane **11**. The spiroketal subunit of bistramide A was modified at the C39-alcohol to give another point of stereochemical diversification. The fragments were coupled by using a standard peptide coupling protocol to provide 35 stereoisomers of the natural product. These stereochemical analogues were screened for their effects on cellular actin and cytotoxicity against cancer cell lines (UO-31 renal and SF-295 CNS). The results of these assays identified one analogue, **1.21**, with enhanced potency relative to the natural product, bistramide A.

### Introduction

Actin is a cytoskeletal protein that plays a crucial role in maintenance of cell shape and other important cellular processes including motility, cytokinesis, phagocytosis, and intracellular transport. These functions are important for normal cell viability as well as for the aberrant processes vital to cancer cell growth, invasion, and metastasis. To function properly, actin is actively switched in a dynamic equilibrium between the G-actin and F-actin, both targets of natural products.<sup>1</sup> The complex nature of actin regulation is under active investigation, and cell signaling pathways that include the small GTPases Rho, Rac, and Cdc42 have been found to play coordinated, important roles in the assembly and disassembly of actin-rich structures such as stress fibers, lamellipodia, filopodia, and focal adhesion complexes.<sup>1</sup>

While drugs that directly modulate actin have not progressed to the stage of use as clinical cancer therapeutics, actin inhibitors have demonstrated activity in many in vitro cancer models. In addition, actin inhibitors have been extremely useful in elucidating the role of actin in cellular processes. Natural products, in particular, have been a rich source of actin inhibitors, and many have been cocrystallized with actin.<sup>2</sup> The cytochalasins and phalloidins bind to F-actin,<sup>2</sup> while G-actin modulators include latrunculins, mycalolide B, jasplakinolide, dolastatin 11, aplyronine A, swinholide A, and bistramide A.<sup>3</sup> Of the latter group, bistramide A is unique in its binding mode to actin. Bistramide A binds and sequesters G-actin and thus inhibits actin filament formation, thereby promoting filament disruption.<sup>4</sup> A high-resolution X-ray crystallographic structure of the bistramide A–actin complex showed its binding site overlaps only slightly

<sup>†</sup> Boston University.

<sup>‡</sup> NCI at Frederick.

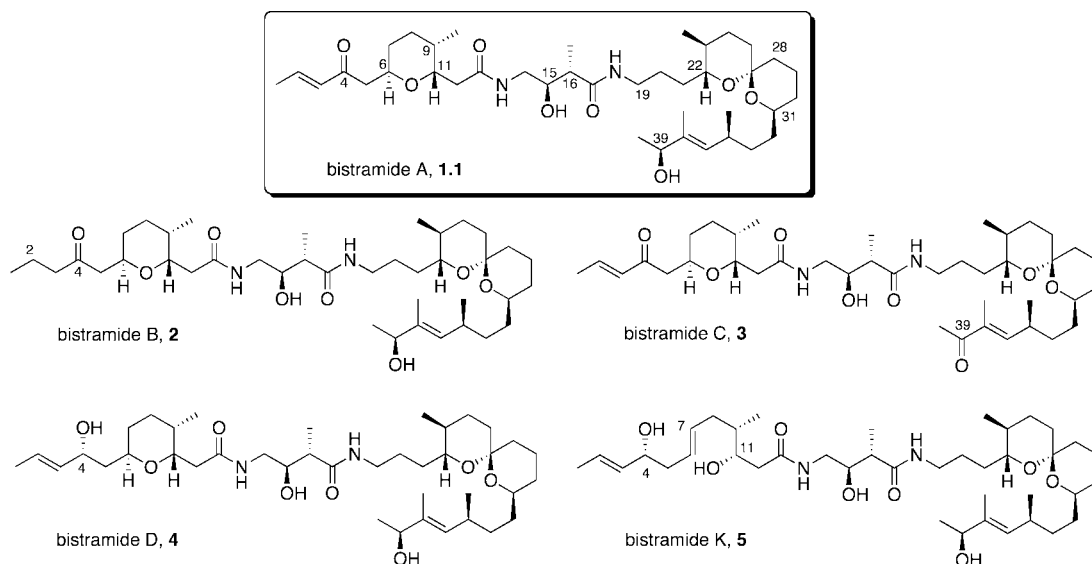
<sup>§</sup> SAIC-Frederick.

(1) Nobes, C. D.; Hall, A. *Cell* **1995**, *81*, 53.

(2) Cooper, J. A. *J. Cell Biol.* **1987**, *105*, 1473.

(3) (a) Allingham, J. S.; Klenchin, V. A.; Rayment, I. *Cell. Mol. Life Sci.* **2006**, *63*, 2119. (b) Saito, S.; Watabe, S.; Ozaki, H.; Kigoshi, H.; Yamada, K.; Fusetani, N.; Karaki, H. *J. Biochem.* **1996**, *120*, 552. (c) Bubb, M. R.; Spector, I.; Bershadsky, A. D.; Korn, E. D. *J. Biol. Chem.* **1995**, *270*, 3463.

## SCHEME 1. Structures of Bistramides A–D and K



with that of other G-actin inhibitors.<sup>5</sup> Thus, bistramide A is a novel actin inhibitor worthy of further investigation.

Stereochemically complex natural products provide an opportunity to discover novel biologically relevant molecules. Variation of chirality at selected stereocenters presents a method for diversifying natural products as library templates or scaffolds.<sup>6</sup> Each member of a stereoisomer library should provide a unique conformational profile that could have a substantial effect on the biological activity. It is well documented that a conformation of a molecule often modulates specific interactions with its biological target, either to enhance or attenuate biological activity. The so-called stereostructure/activity relationships (SSAR) have only recently gained attention with respect to complex natural products.<sup>6b</sup> Our group has developed and explored the utility of chiral organosilane reagents to prepare stereochemically well-defined and diversified intermediates for natural product synthesis. Having access to stereochemical iterations of these building blocks presents the opportunity to construct multiple conformations of complex natural products. In this article, we report preparation and use of these chiral reagents to synthesize, in solution phase, a focused 35-member library of the marine metabolite bistramide A **1.1**, and the associated biology of these new compounds.

In 1988, Verbist and co-workers isolated the highly potent antiproliferative agent bistramide A, **1.1**, from the marine ascidian *Lissoclinium bistratum*.<sup>7</sup> Four additional congeners of this class of natural products were reported by the same research group in 1994.<sup>8</sup> The structure of bistramide A was originally proposed to be a 19-membered macrolactam<sup>9</sup> but later revised to a linear carbon framework (Scheme 1).<sup>10</sup> The skeletal architecture of bistramide A consists of a substituted tetrahy-

dropyran and a spiroketal subunit joined at the center by a  $\gamma$ -amino acid linker. Subsequent spectroscopic and computational studies allowed for accurate prediction of relative and absolute configurations of bistramides.<sup>11</sup> Kozmin reported the first total synthesis of bistramide A in 2004, which confirmed the proposed stereostructure of the natural product.<sup>12</sup> To date, there are several reports detailing fragment,<sup>11b,13</sup> degradative,<sup>11a,14</sup> and total syntheses<sup>15</sup> of bistramides A–D and K.

In addition to the structural<sup>9–11</sup> and synthetic challenges posed by this family of natural products, numerous reports describing their diverse bioactivity have recently emerged.<sup>16</sup> Bistramides were shown to exhibit various biological activities, encompassing neurotoxic,<sup>7b</sup> antiproliferative,<sup>16d</sup> and cytotoxic properties.<sup>7b,8</sup> Specifically, bistramide A displayed activity against a number of tumor cell lines including KB, P388, P388/dox, B16, HT29, and NSCLC-N6 cell lines with IC<sub>50</sub> values in the 0.03–0.32  $\mu\text{g}/\text{mL}$  range.<sup>16a</sup> The antiproliferative activity of bistramide A

(8) Biard, J.-F.; Roussakis, C.; Kornprobst, J.-M.; Gouiffès-Barbin, D.; Verbist, J.-F.; Cotellet, P.; Foster, M. P.; Ireland, C. M.; Debitus, C. *J. Nat. Prod.* **1994**, *57*, 1336.

(9) Degnan, B. M.; Hawkins, C. J.; Lavin, M. F.; McCaffrey, E. J.; Parry, D. L.; Watters, D. J. *J. Med. Chem.* **1989**, *32*, 1354.

(10) Foster, M. P.; Mayne, C. L.; Dunkel, R.; Pugmire, R. J.; Grant, D. M.; Kornprobst, J. M.; Verbist, J. F.; Biard, J. F.; Ireland, C. M. *J. Am. Chem. Soc.* **1992**, *114*, 1110.

(11) (a) Solladié, G.; Baudet, C.; Biard, J. F. *Tetrahedron Lett.* **2000**, *41*, 7747. (b) Gallagher, P. O.; McErlean, C. S. P.; Jacobs, M. F.; Watters, D. J.; Kitching, W. *Tetrahedron Lett.* **2002**, *43*, 531. (c) Wipf, P.; Uto, Y.; Yoshimura, S. *Chem. Eur. J.* **2002**, *8*, 1670. (d) Zuber, G.; Goldsmith, M.-R.; Hopkins, T. D.; Beratan, D. N.; Wipf, P. *Org. Lett.* **2005**, *7*, 5269. (e) Hiebel, M.-A.; Pelotier, B.; Lhoste, P.; Piva, O. *Synlett* **2008**, 1202.

(12) Statsuk, A. V.; Liu, D.; Kozmin, S. A. *J. Am. Chem. Soc.* **2004**, *126*, 9546.

(13) Lowe, J. T.; Panek, J. S. *Org. Lett.* **2005**, *7*, 3231.

(14) Bauder, C.; Biard, J.-F.; Solladié, G. *Org. Biomol. Chem.* **2006**, *4*, 1860.

(15) (a) Yadav, J. S.; Chetia, L. *Org. Lett.* **2007**, *9*, 4587. (b) Lowe, J. T.; Wrona, I. E.; Panek, J. S. *Org. Lett.* **2007**, *9*, 327. (c) Crimmins, M. T.; DeBaillie, A. C. *J. Am. Chem. Soc.* **2006**, *128*, 4936. (d) Wipf, P.; Hopkins, T. D. *Chem. Commun.* **2005**, 3421.

(16) (a) Johnson, W. E. B.; Watters, D. J.; Suniara, R. K.; Brown, G.; Bunce, C. M. *Biochem. Biophys. Res. Commun.* **1999**, *260*, 80. (b) Gautret, P.; Le Pape, P.; Biard, J. F.; Menard, D.; Verbist, J. F.; Marjolet, M. *Acta Parasitol.* **1998**, *43*, 50. (c) Pusset, J.; Maillere, B.; Debitus, C. *J. Nat. Toxins* **1996**, *5*, 1. (d) Riou, D.; Roussakis, C.; Robillard, N.; Biard, J. F.; Verbist, J. F. *Biol. Cell* **1993**, *77*, 261. (e) Sauviat, M. P.; Verbist, J. F. *Gen. Physiol. Biophys.* **1993**, *12*, 465. (f) Sauviat, M. P.; Chesnais, J. M.; Choukri, N.; Diacono, J.; Biard, J. F.; Verbist, J. F. *Cell Calcium* **1993**, *14*, 301. (g) Sauviat, M. P.; Gouiffès-Barbin, D.; Ecault, E.; Verbist, J. F. *Biochim. Biophys. Acta, Biomembranes* **1992**, *1103*, 109.

(4) Statsuk, A. V.; Bai, R.; Baryza, J. L.; Verma, V. A.; Hamel, E.; Wender, P. A.; Kozmin, S. A. *Nat. Chem. Biol.* **2005**, *1*, 383.

(5) Rizvi, S. A.; Tereshko, V.; Kossiakoff, A. A.; Kozmin, S. A. *J. Am. Chem. Soc.* **2006**, *128*, 3882.

(6) (a) Zhang, Q.; Lu, H.; Richard, C.; Curran, D. P. *J. Am. Chem. Soc.* **2004**, *126*, 36. (b) Curran, D. P.; Zhang, Q.; Richard, C.; Lu, H.; Gudipati, V.; Wilcox, C. S. *J. Am. Chem. Soc.* **2006**, *128*, 9561. (c) Dandapani, S.; Jeske, M.; Curran, D. P. *J. Org. Chem.* **2005**, *70*, 9447.

(7) (a) Gouiffès, D.; Moreau, S.; Helbecque, N.; Bernier, J. L.; Hénichart, J. P.; Barbin, Y.; Laurent, D.; Verbist, J. F. *Tetrahedron* **1988**, *44*, 451. (b) Gouiffès, D.; Juge, M.; Grimaud, N.; Welin, L.; Sauviat, M. P.; Barbin, Y.; Laurent, D.; Roussakis, C.; Henichart, J. P.; Verbist, J. F. *Toxicol.* **1988**, *26*, 1129.

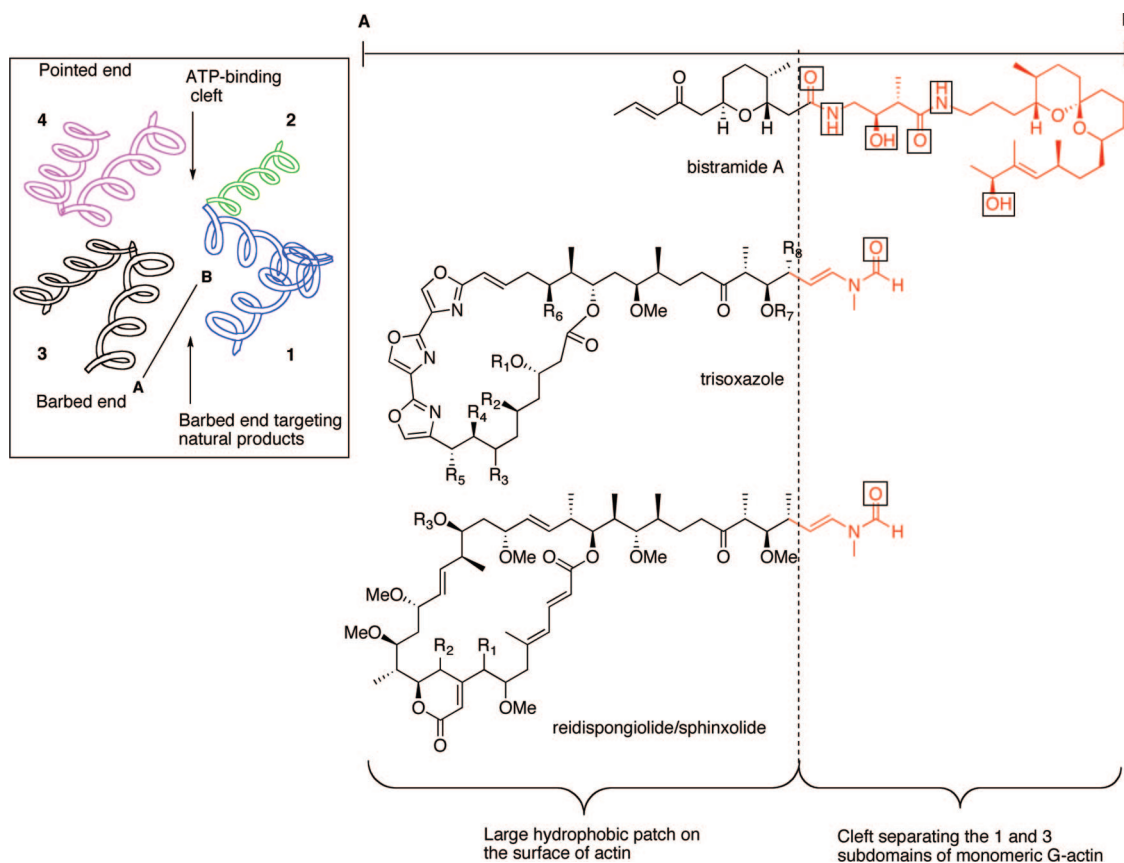


**FIGURE 1.** A schematic drawing of the actin monomer showing the major subdomains (inset). Cross-section representation of **1** and **3** subdomains of G-actin. The red portion of the molecules insert into the “cleft” of **1** and **3** subdomains of actin. The atoms of the natural products involved in polar contacts with the protein are boxed.

was initially hypothesized to be due to selective activation of protein kinase C- $\delta$ .<sup>17</sup> In 2006, however, Kozmin and co-workers obtained a crystal structure of the natural product bound to a single monomeric unit of G-actin.<sup>4,5,18</sup> actin is a 43 kDa protein consisting of four subdomains. ATP and  $Mg^{2+}$  bind within a deep cleft between subdomains 4 and 2 and polymerization occurs asymmetrically at the pointed and barbed ends of the monomer with 5-times greater polymerization occurring at the pointed end. For natural products known to target actin directly, the barbed end and the ATP-binding domain are the primary sites of interaction. Bistramide A belongs to the class of natural products that induce disassembly of microfilaments (or prevent its formation) by interfering with the barbed end of the actin monomer (inset, Figure 1). Within the bistramide A binding pocket of actin, an intimate hydrogen bonding network was observed between the protein and the central amino acid portion of the molecule. In contrast to bistramide A, however, most barbed end targeting molecules such as reidispongiolides,<sup>19</sup> sphinxolides,<sup>19</sup> trisoxazoles,<sup>20</sup> and others<sup>21</sup> have very few polar

contacts within the actin pocket. The cross-sectional representation of the 1 and 3 subdomains of G-actin shows the difference in binding between bistramide A and other natural products (Figure 1). The binding of most actin targeting natural products relies mainly on hydrophobic interactions between their respective macrocycles and a shallow patch on the side of actin.<sup>3a</sup> Bistramide A, on the other hand, inserts deep into the pocket and displays multiple polar contacts, thus allowing for a unique binding mode among barbed end targeting natural products.<sup>22</sup>

With a detailed model in hand, the present study examines the biological and conformational effects of specific stereoisomers of bistramide A.<sup>23</sup> These epimers incorporate small, subtle changes into a highly organized system, allowing us to determine the importance of each polar contact as well as how the stereochemical environment associated with these contacts defines changes in biological activity and conformation within the actin pocket. The notable differences in the way bistramide A binds to actin through a highly ordered hydrogen bonding network and few stereostructural activity relationship (SSAR) studies for this specific class of molecules supports the relevance of this study. By systematically altering the stereochemical environment of this highly conserved portion of the molecule, a framework is provided for designing potentially more potent analogues of bistramide A.

(17) Griffiths, G.; Garrone, B.; Deacon, E.; Owen, P.; Pongracz, J.; Mead, G.; Bradwell, A.; Watters, D.; Lord, J. *Biochem. Biophys. Res. Commun.* **1996**, *222*, 802.

(18) Rizvi, S. A.; Courson, D. S.; Keller, V. A.; Rock, R. S.; Kozmin, S. A. *Proc. Natl. Acad. Sci. U.S.A.* **2008**, *105*, 4088.

(19) Allingham, J. S.; Zampella, A.; D'Auria, M. V.; Rayment, I. *Proc. Natl. Acad. Sci. U.S.A.* **2005**, *102*, 14527.

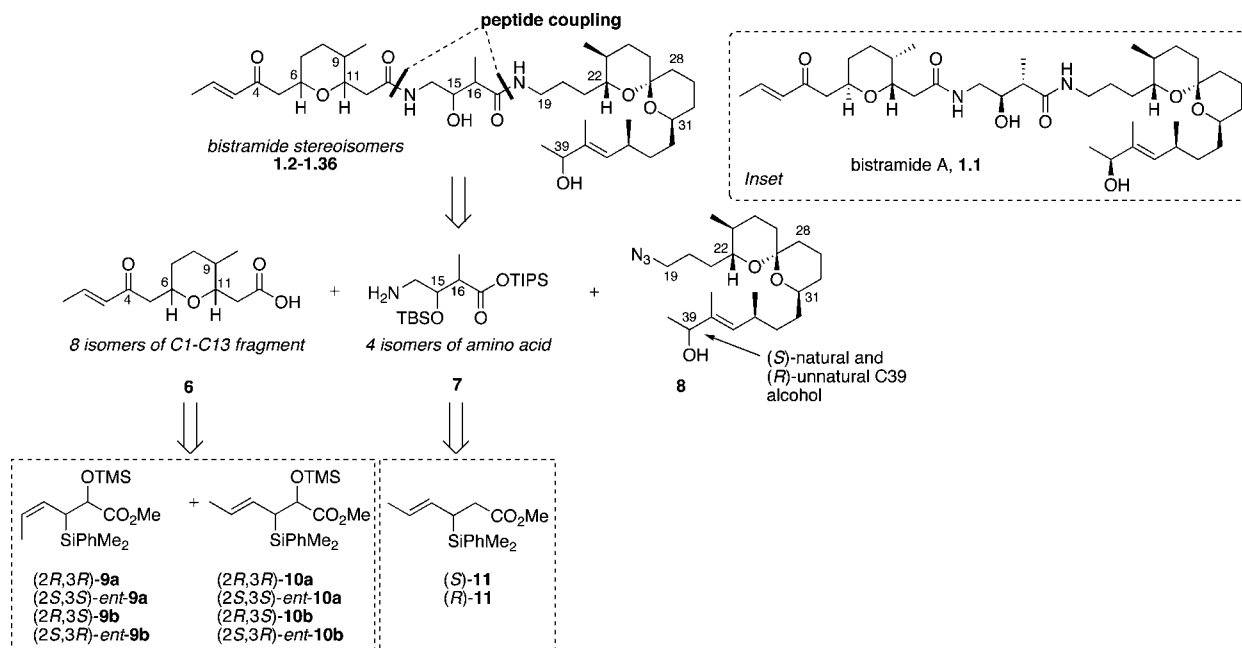
(20) Klenchin, V. A.; Allingham, J. S.; King, R.; Tanaka, J.; Marriott, G.; Rayment, I. *Nat. Struct. Biol.* **2003**, *10*, 1058.

(21) (a) Hirata, K.; Muraoka, S.; Suenaga, K.; Kuroda, T.; Kato, K.; Tanaka, H.; Yamamoto, M.; Takata, M.; Yamada, K.; Kigoshi, H. *J. Mol. Biol.* **2006**, *356*, 945. (b) Klenchin, V. A.; King, R.; Tanaka, J.; Marriott, G.; Rayment, I. *Chem. Biol.* **2005**, *12*, 287.

(22) For a review see: (a) Yeung, K. S.; Paterson, I. *Angew. Chem., Int. Ed.* **2002**, *41*, 4632. (b) Spector, I.; Braet, F.; Shochet, N. R.; Bubb, M. R. *Microsc. Res. Tech.* **1999**, *47*, 18. (c) Fenteany, G.; Zhu, S. *Curr. Top. Med. Chem.* **2003**, *3*, 593.

(23) For structural activity relationship studies on bistramide A, see ref 18.

## SCHEME 2. Retrosynthetic Analysis of Bistramide Stereoisomers 1.1–1.36



Our initial interest was focused on reported points of hydrogen bonding (C13, C13–N, C15, C18, C18–N, C39) of the molecule and how subtle stereochemical changes would affect the overall activity of bistramide A. Next, we considered the stereochemical environment around the tetrahydropyran where hydrophobic interactions are thought to play an important role between bistramide A and the actin pocket. A recent account has explored these potential binding sites through computational measurements and highlighted the importance of tetrahydropyran fragment in regards to binding and cytotoxicity.<sup>24</sup> A greater understanding of such molecular systems may allow for design and synthesis of more efficacious anticancer agents. Herein, we report the synthesis and the associated biological activity of 35 stereoisomers of the bistramide A planar structure.

## Results/Discussion

**Retrosynthetic Analysis.** Recently, we reported a total synthesis of bistramide A that utilizes 21 steps (longest linear sequence) from readily available reagents.<sup>15b</sup> The strategy was highlighted by the use of three different chiral crotylsilane reagents to construct all principle fragments [(6*R*,9*S*,11*R*)-**6**, (15*S*,16*R*)-**7**, and (39*S*)-**8**] and simultaneously install 8 of 11 stereogenic centers. Following our reported synthesis, we decided to make several stereochemical iterations (35) of the natural product in order to conduct SSAR studies. While synthesis of this many stereoisomers of a complex natural product might seem daunting, the highly convergent nature of the synthesis together with ready access to a wide range of chiral organosilane reagents greatly simplified the strategic plan. Accordingly, disconnection at the amide bonds provided three fragments of varying size and complexity possessing different synthetic challenges (Scheme 2). The eight stereoisomers of pyran **6** were envisioned to come from (*E*)- and (*Z*)-crotylsilane reagents **9** and **10**. This is the first example of using one methodology to access all possible stereoisomers of a 2,5,6-

substituted tetrahydropyran system. The four isomers of the central amino acid portion **7** were anticipated to arise from Lewis acid-mediated additions using chiral (*E*)-silane reagents **11**. The spiroketal fragment, at the present time, was envisioned to remain stereostructurally intact except for the C39 alcohol. Enantioselective reduction of the precursor  $\alpha,\beta$ -unsaturated ketone with CBS reagent allowed for formation of the unnatural C39-epimer.

**Preparation of All Stereochemical Permutations of C1–C13 Fragment 6.** Recent accounts from our group detailed formal [4+2]-annulations of enantioenriched allyl- and crotylsilanes with aldehydes to form highly functionalized dihydropyran systems.<sup>25</sup> This methodology was applied to the synthesis of complex natural products, including (–)-apicularen A, (+)-leucascandrolide A, callipeltoside A, GEX 1A, (+)-neopeltolide, and most recently kendomycin.<sup>26</sup> To synthesize bistramide A, the then currently available silane reagents did not allow direct access to the C9–C11-*cis* configuration of the pyran moiety. This can be explained by inspecting the proposed mechanism of (*E*)-*anti*-crotylsilane *ent*-**10b** (Scheme 3). The absolute stereochemical outcome of the annulation reaction has been proposed to occur via an intramolecular *anti*-S<sub>E</sub>' mode of addition.<sup>27</sup>

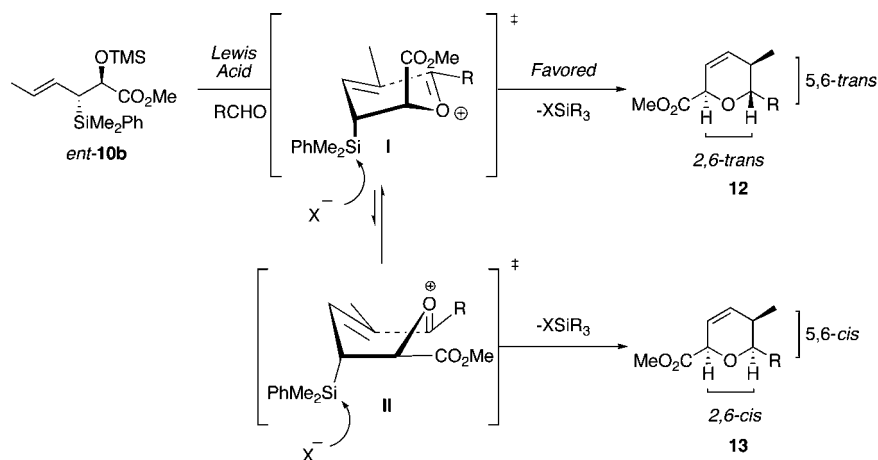
The crotylsilane reagent *ent*-**10b** will react with an aldehyde in the presence of a Lewis acid, forming a mixed acetal that eventually leads to generation of an oxocarbenium ion **I**. This reactive intermediate, if placed in a chairlike transition state with the silyl group in a pseudoaxial orientation, allows for the most effective orbital  $\sigma_{C-Si}-\pi$  overlap and stabilization of the adjacent positive charge ( $\beta$ -effect). Electrophilic cyclization and elimination of silicon group provides the 2,6-*trans*-5,6-*trans*-dihydropyran **12** as the major diastereomer. To obtain the 5,6-

(25) Huang, H.; Panek, J. S. *J. Am. Chem. Soc.* **2000**, *122*, 9836.

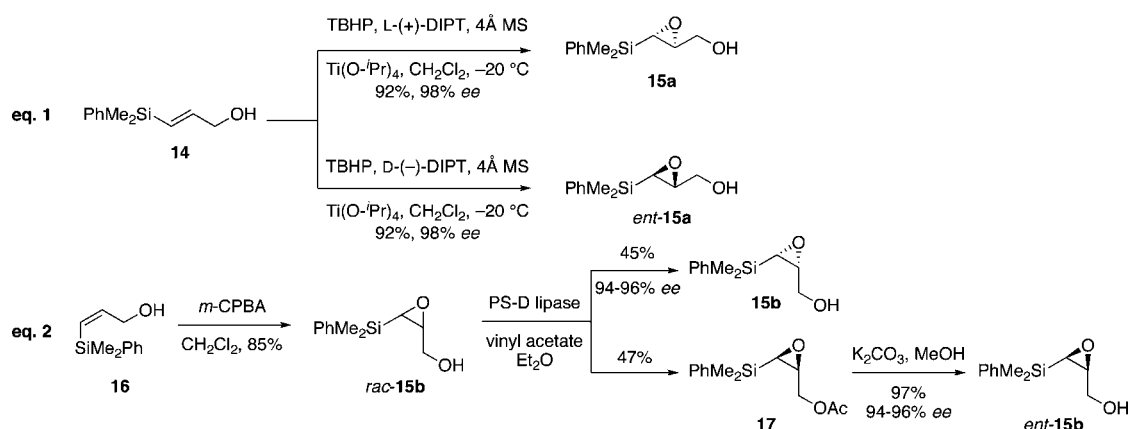
(24) Melville, J. L.; Moal, I. H.; Baker-Glenn, C.; Shaw, P. E.; Pattenden, G.; Hirst, J. D. *Biophys. J.* **2007**, *92*, 3862.

(26) (a) Huang, H.; Panek, J. S. *Org. Lett.* **2004**, *6*, 4383. (b) Su, Q.; Panek, J. S. *J. Am. Chem. Soc.* **2004**, *126*, 2425. (c) Su, Q.; Dakin, L.; Panek, J. S. *J. Org. Chem.* **2007**, *72*, 2. (d) Zhang, Y.; Panek, J. S. *Org. Lett.* **2007**, *9*, 3141. (e) Youngsaye, W.; Lowe, J. T.; Pohlki, F.; Ralifo, P.; Panek, J. S. *Angew. Chem., Int. Ed.* **2007**, *46*, 9211. (f) Lowe, J. T.; Panek, J. S. *Org. Lett.* **2008**, *10*, 3813. (27) Masse, C. E.; Panek, J. S. *Chem. Rev.* **1995**, *95*, 1293.



SCHEME 3. Proposed Mechanism for Formation of 2,6-*trans*-5,6-*trans*-Dihydropyran 12

## SCHEME 4. Preparation of Enantiomers of Silyl glycidols



*cis* configuration needed for bistramide A, however, the reaction would have to proceed through a boat-like conformation **II**. This alternate transition state suffers from a number of destabilizing interactions that provide 2,6-*cis*-5,6-*cis*-dihydropyran **13** only as the minor product.

To utilize organosilane-based [4+2]-annulation methodology to construct the C1–C13 portion of bistramide A, a new crotylsilane reagent was required. We reasoned, based on the proposed transition state, that changing olefin geometry from (*E*) to (*Z*) could effectively allow access to the desired 5,6-*cis*-dihydropyrans (minor isomer **13** in Scheme 3). The outlined annulation approach would create a complementary reagent to our well-established methodologies.

The (*E*)-*syn* and (*E*)-*anti* organosilane reagents **10** were obtained through various Claisen rearrangement strategies.<sup>28</sup> Preparation of the proposed (*Z*)-crotylsilane reagent **9** with these rearrangement reactions was anticipated to be problematic due to potential olefin isomerization. What was required was a route that would allow access to all structural and stereochemical variations of this new reagent. Inspired by a recent review,<sup>29</sup> we hoped epoxysilanes **15** would provide enantioenriched crotylsilanes **9**. Epoxysilanes are known for their ease of preparation and serve as versatile building blocks and synthetic intermediates.<sup>30</sup> Methods to generate these substrates in their

enantioenriched form are also available.<sup>31</sup> The general interest in epoxysilanes stems from their predictable behavior in nucleophilic oxirane openings to provide a wide range of functionalized  $\beta$ -hydroxysilanes.<sup>32</sup>

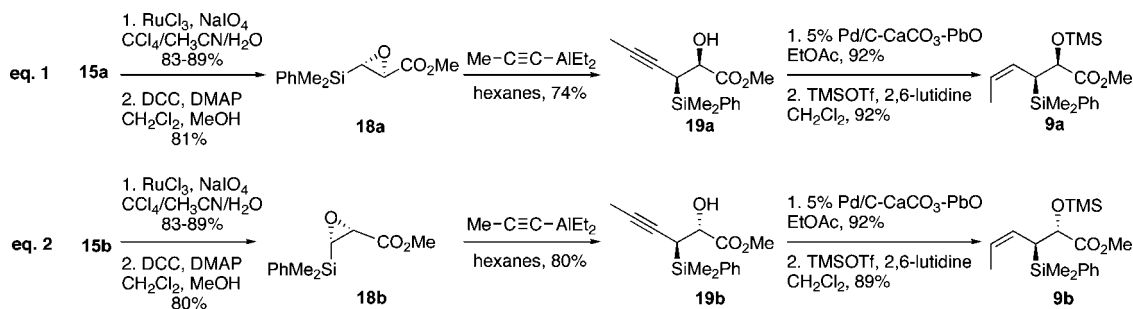
Preparation of *cis*- and *trans*-epoxysilanes required for synthesis of enantioenriched (*Z*)-crotylsilanes is depicted in Scheme 4. As anticipated, the *trans*-silyl glycidols **15a** were obtained from a modified Sharpless asymmetric epoxidation of (*E*)-vinylsilane **14** with (+)- or (–)-diethyl tartrate, respectively.<sup>33</sup> The resulting epoxysilyl alcohols **15a** and *ent*-**15a** were produced in 87% yield (2 steps from propargyl alcohol) and with >98% enantiomeric excess (eq 1 in Scheme 4).<sup>34</sup> A similar multigram synthesis of a derivative of enantioenriched epoxysilane **15a** was previously reported.<sup>35</sup>

(30) (a) Chakraborty, T. K.; Laxman, P. *Tetrahedron Lett.* **2003**, *44*, 4989. (b) Hudrlík, P. F.; Gebreselassie, P.; Tafesse, L.; Hudrlík, A. M. *Tetrahedron Lett.* **2003**, *44*, 3409. (c) Kim, K.; Okamoto, S.; Takayama, Y.; Sato, F. *Tetrahedron Lett.* **2002**, *43*, 4237. (d) Whitham, G. H. *Sci. Synth.* **2002**, *4*, 633. (e) Babudri, F.; Fiandanese, V.; Marchese, G.; Punzi, A. *Tetrahedron* **2001**, *57*, 549. (f) Chakraborty, T. K.; Reddy, G. V. *Tetrahedron Lett.* **1990**, *31*, 1335.

(31) For examples of Sharpless asymmetric epoxidation to generate epoxysilanes see: (a) Chauret, D. C.; Chong, J. M.; Ye, Q. *Tetrahedron: Asymmetry* **1999**, *10*, 3601. (b) Kobayashi, Y.; Ito, T.; Yamakawa, I.; Urabe, H.; Sato, F. *Synlett* **1991**, 811. (c) Takeda, Y.; Matsumoto, T.; Sato, F. *J. Org. Chem.* **1986**, *51*, 4728. For an example of Shi epoxidation see: (d) Heffron, T. P.; Jamison, T. F. *Org. Lett.* **2003**, *5*, 2339. For examples of kinetic resolutions see: (e) Carlier, P. R.; Mungall, W. S.; Schroder, G.; Sharpless, K. B. *J. Am. Chem. Soc.* **1988**, *110*, 2978. (f) Kitano, Y.; Matsumoto, T.; Sato, F. *J. Chem. Soc., Chem. Commun.* **1986**, *17*, 1323. For substrate directed epoxidations using VO(acac)<sub>2</sub> see: (g) Kobayashi, Y.; Uchiyama, H.; Kanbara, H.; Sato, F. *J. Am. Chem. Soc.* **1985**, *107*, 5541.

(28) (a) Sparks, M. A.; Panek, J. S. *J. Org. Chem.* **1991**, *56*, 3431. (b) Panek, J. S.; Yang, M. *J. Org. Chem.* **1991**, *56*, 5755. (c) Panek, J. S.; Clark, T. D. *J. Org. Chem.* **1992**, *57*, 4323.

(29) Hudrlík, P. F.; Hudrlík, A. M. *Advances in Silicon Chemistry*; JAI Press: Greenwich, CT, 1993; Vol. 2, p 1.

SCHEME 5. Synthesis of (*Z*)-Crotylsilanes **9**

Generation of the *cis*-epoxysilanes **15b** and *ent*-**15b** was initially attempted with enantioselective epoxidation of the complementary (*Z*)-vinylsilane **16**. Subjection of this silane **16** to Sharpless asymmetric epoxidation resulted in production of the desired product in less than 5% yield.<sup>36</sup> Accordingly, we explored the possibility of an enzymatic resolution of the racemic epoxide (eq 2 in Scheme 4).<sup>37</sup> Epoxidation of vinylsilanes **16** with *m*-CPBA gave a racemic mixture of epoxy alcohols *rac*-**15b** in 85% yield. Several lipase enzymes were surveyed to resolve the racemate.<sup>38</sup> Best results were obtained by using Amano PS-D lipase in the presence of vinyl acetate to provide primary alcohol **15b** and acetate **17** in high yields and enantiomeric excess. Base-catalyzed methanolysis of the acetate group gave the desired *cis*-epoxysilane *ent*-**15b** in 97% yield.<sup>39</sup> To the best of our knowledge this is the first example of enzymatically resolved silylglycidols.

A straightforward, 3-step sequence of oxidation, oxirane opening, and Lindlar reduction was used for completion of the (*Z*)-crotylsilane reagent **9** (Scheme 5). Primary alcohol **15a** was subjected to NaIO<sub>4</sub> and catalytic RuCl<sub>3</sub><sup>40</sup> to give an acid, which was immediately esterified<sup>41</sup> with DCC to provide *trans*-silyl glycidate **18a** (72%, 2 steps). Applying the oxidation/esterification sequence to the *cis*-epoxide **15b** proved troublesome. Upon scale-up, a significant amount of aldehyde was observed (ca. 20%) resulting in a two-step 55% isolated yield for ester **18b**. Fortunately, two sequential catalytic ruthenium oxidations<sup>42</sup> followed by esterification with DCC/DMAP afforded the silyl

glycidate **18b** in 66% yield over 2 steps. Both the *cis*- and *trans*-silylglycidates **18** have been prepared in >25 g quantities.

Regioselective epoxide ring opening with diethylpropynylaluminum<sup>30c</sup> gave 2,3-*syn*- and 2,3-*anti*-hexyne methyl esters **19a** and **19b**, respectively, in moderate yields and good selectivities. Minor reaction byproducts included alkyne addition to the methyl ester and chloride opening of the silyl glycidate. The latter is a common byproduct obtained from metal additions to epoxysilanes (e.g., Grignard).<sup>29</sup> Fortunately, addition of the alkyne to the  $\beta$ -carbon of the silicon functionality was not detected in the described conditions. Several explanations have been put forth on the selective opening of epoxysilanes.<sup>29,43–45</sup> One interesting hypothesis includes the formation of a penta-coordinated silicon followed by 1,2-migration,<sup>45</sup> though more recent studies with allyl cuprates do not support this pathway.<sup>43</sup> Alternatively, prior coordination of nucleophile with both the R-carbon and silicon functionality has also been postulated.<sup>44</sup> Lastly, X-ray crystal structure<sup>46</sup> and gas phase and theoretical studies<sup>47</sup> showed the  $\alpha$  C–O bond (adjacent to the Si) to be longer and weaker than the  $\beta$  C–O bond. Our particular system has the added advantage of a Lewis basic site on the adjacent carbonyl to aid in opening via coordination of resident metal centers. Lindlar reduction of alkynes **19** followed by protection of the secondary alcohols as their TMS ethers gave the *syn*- and *anti*-(*Z*)-crotylsilanes **9a** and **9b** and their enantiomers. Each stereoisomer was prepared in >10 g quantities.

The preparation of the required 5,6-*cis*-dihydropyran of the C1–C13 fragment of bistramide A was explored next. Recently, we described a [4+2]-annulation of *syn*-(*Z*)-crotylsilane reagent **9a** with  $\beta$ -benzyloxy aldehyde **20** to provide the desired 5,6-*cis*-pyran **21a** in 66% yield (Table 1, entry 1). Extension of this methodology to the other isomer silanes would afford all possible stereochemical iterations of 2,5,6-dihydropyrans. Subjection of all *syn*- and *anti*-(*Z*)- and (*E*)-silane reagents **9** and **10** to aldehyde **20**<sup>48</sup> under TMSOTf-catalyzed conditions afforded the eight possible stereochemical analogues of the

(42) During the course of oxidation, the reaction solution became a dark green color with a black suspension, suggesting an inactive catalytic system. To drive the reaction to completion, catalyst loading was increased and extended reaction times were explored with little success. Only a reset of the catalytic system provided full conversion.

(43) Hudrlík, P. F.; Ma, D.; Bhamidipati, R. S.; Hudrlík, A. M. *J. Org. Chem.* **1996**, *61*, 8655.

(44) (a) Eisch, J. J.; Galle, J. E. *J. Org. Chem.* **1976**, *41*, 2615. (b) Eisch, J. J.; Trainor, J. T. *J. Org. Chem.* **1963**, *28*, 2870.

(45) (a) Davis, A. P.; Hughes, G. J.; Lowndes, P. R.; Robbins, C. M.; Thomas, E. J.; Whitham, G. H. *J. Chem. Soc., Perkin Trans.* **1981**, *1*, 1934. (b) Eisch, J. J.; Chiu, C. S. *J. Organomet. Chem.* **1988**, *358*, C1.

(46) Siriwardane, U.; Chu, S. S. C.; Buynak, J. D. *Acta Crystallogr., Sect. C: Cryst. Struct. Commun.* **1989**, *C45*, 531.

(47) Fristad, W. E.; Bailey, T. R.; Paquette, L. A.; Gleiter, R.; Boehm, M. C. *J. Am. Chem. Soc.* **1979**, *101*, 4420.

(48) Cloarec, J.-M.; Charette, A. B. *Org. Lett.* **2004**, *6*, 4731.

(32) (a) Adam, J.-M.; de Fays, L.; Laguerre, M.; Ghosez, L. *Tetrahedron* **2004**, *60*, 7325. (b) Landais, Y.; Mahieux, C.; Schenk, K.; Surange, S. S. *J. Org. Chem.* **2003**, *68*, 2779. (c) Ohi, H.; Inoue, S.; Iwabuchi, Y.; Irie, H.; Hatakeyama, S. *Synlett* **1999**, *11*, 1757. (d) Fleming, I.; Barbero, A.; Walter, D. *Chem. Rev.* **1997**, *97*, 2063. (e) Chauret, D. C.; Chong, J. M. *Tetrahedron Lett.* **1993**, *34*, 3695. (f) Russell, A. T.; Procter, G. *Tetrahedron Lett.* **1987**, *28*, 2041. (g) Tamao, K.; Nakajo, E.; Ito, Y. *J. Org. Chem.* **1987**, *52*, 4412. (h) Hudrlík, P. F.; Peterson, D.; Rona, R. J. *J. Org. Chem.* **1975**, *40*, 2263.

(33) Gao, Y.; Hanson, R. M.; Klunder, J. M.; Ko, S. Y.; Masamune, H.; Sharpless, K. B. *J. Am. Chem. Soc.* **1987**, *109*, 5765.

(34) Lowe, J. T.; Youngsaye, W.; Panek, J. S. *J. Org. Chem.* **2006**, *71*, 3639. The enantiomeric excess was determined to be 98% for both **15a** and *ent*-**15a** as observed with Chiralcel OD 99/1 (hexanes/IPA) at 1 mL/min (*t<sub>R</sub>* 35:92 for **15a** and 45:17 for *ent*-**15a**).

(35) For preparation of (2*R*,3*R*)-3-(triphenylsilyl)-2,3-epoxypropane-1-ol see: Raubo, P.; Wicha, J. *Tetrahedron: Asymmetry* **1995**, *6*, 577.

(36) Elevated temperatures (−20, 0, and 25 °C) under the described conditions for the (*E*)-vinylsilane did not provide the desired epoxide.

(37) A Shi epoxidation of **16** was also considered; however, literature precedent showed attenuated ee values for similar systems, see ref 32d for more information.

(38) Lipase AK “Amano” 20, Lipase PS “Amano”, and Lipase PS-D “Amano” were initially screened. Lipase PS-D was found to be superior.

(39) The enantiomeric excess was determined to vary between 94% and 96% for both **15b** and *ent*-**15b** as observed with Chiralcel OD 85/15 (hexanes/IPA) at 1 mL/min (*t<sub>R</sub>* 5:03 for **15b** and 7:08 for *ent*-**15b**).

(40) Carlsen, P. H. J.; Katsuki, T.; Martin, V. S.; Sharpless, K. B. *J. Org. Chem.* **1981**, *46*, 3936.

(41) Decomposition of *cis* and *trans* epoxide acids was noticed upon prolonged storage or column chromatography.

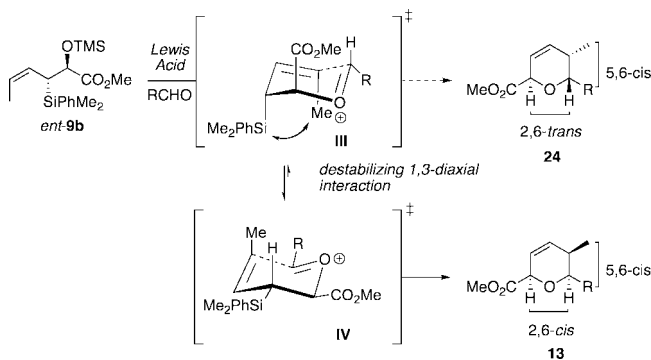
**TABLE 1.** [4+2]-Annulation of both (*Z*)- and (*E*)-Crotylsilanes **9** and **10** with Aldehyde **20**

entry	silane	product <sup>a</sup>	yield <sup>b</sup>	dr <sup>c</sup>
1			66%	12:1
2	<i>ent</i> - <b>9a</b>	<i>ent</i> - <b>21a</b>	63%	12:1
3			60%	15:1
4	<i>ent</i> - <b>9b</b>	<i>ent</i> - <b>21b</b>	63%	15:1
5			78%	20:1
6	<i>ent</i> - <b>10a</b>	<i>ent</i> - <b>21c</b>	72%	20:1
7			50%	1:1
8			53%	4:1
9	<i>ent</i> - <b>22</b>	<i>ent</i> - <b>23</b>	57%	3.5:1

<sup>a</sup> Reactions were performed with 1.0 equiv of silane, 1.0 equiv of aldehyde **20**, and 1.0 equiv of TMSOTf in CH<sub>2</sub>Cl<sub>2</sub> at -50 °C. <sup>b</sup> Isolated yield after SiO<sub>2</sub> chromatography. <sup>c</sup> Ratio determined by <sup>1</sup>H NMR analysis of crude reaction mixtures.

2,5,6-dihydropyran system (Table 1). The 2,3-*syn*-(*Z*)-crotylsilanes **9a** and *ent*-**9a** provided 2,6-*trans*-5,6-*cis*-dihydropyrans **21a** and *ent*-**21a** in useful yields and selectivities (entries 1 and 2). In a complementary fashion, the 2,3-*anti*-(*Z*)-crotylsilanes **9b** and *ent*-**9b** gave rise to dihydropyrans **21b** and *ent*-**21b** bearing all *cis*-2,5,6-stereochemical relationships in equally good yields and selectivities (entries 3 and 4). Similarly, the 2,3-*syn*-(*E*)-crotylsilanes **10a** and *ent*-**10a** yielded 2,6-*cis*-5,6-*trans*-dihydropyrans **21c** and *ent*-**21c** with excellent yields and selectivities (entries 5 and 6). The 2,3-*anti*-(*E*)-crotylsilane **10b** underwent annulation to provide dihydropyran **21d** in moderate yield, but with a 1:1 mixture of diastereomers (entry 7). This result, however, was not entirely surprising. A similar problem was encountered during a second generation approach to a late-stage intermediate of leucascandrolide A.<sup>26c</sup> Annulations with 2,3-*anti*-(*E*)-crotylsilane **10b** and protected 3-hydroxypropionaldehyde derivatives provided dihydropyran products in poor yields and selectivities. The problem was addressed through modification of the organosilane reagents to affect the resident A values of the postulated intermediate oxocarbenium ion. This analysis was loosely based on the A values of ethyl (1.1 kcal/mol) versus that of a methyl ester (1.3 kcal/mol) of a mono-substituted cyclohexane ring.<sup>49</sup> The 0.2 kcal/mol difference between methyl and ethyl esters should translate into even higher activation energy for the isopropyl ester. Experimentally,

(49) Smith, M. B.; March, J. *Advanced Organic Chemistry*; John Wiley and Sons: New York, 2001, 5th ed.; p 174.

**SCHEME 6.** Possible Mechanism for (*Z*)-Crotylsilane *ent*-**9b**

annulation of isopropyl ester *anti*-(*E*)-crotylsilanes **22** and *ent*-**22** afforded a 2-fold increase in selectivity for the desired 2,6-*trans*-5,6-*trans*-dihydropyrans **23** and *ent*-**23** (entries 8 and 9).

The stereochemical outcome of the annulation reaction with (*Z*)-crotylsilanes was not entirely anticipated. In sharp contrast to the proposed mechanism of (*E*)-crotylsilanes (Scheme 3), the silyl group of (*Z*)-crotyl reagents presumably adopts a pseudo-equatorial orientation. The oxocarbenium ion of *ent*-**9b** prefers the chairlike intermediate **IV** to give dihydropyran **13** as the major diastereomer (Scheme 6).<sup>50</sup> The potential A<sup>1,3</sup> destabilizing interactions arising from the (*Z*)-olefin and axial silicon in **III**<sup>51</sup> prevent formation of the 2,6-*trans*-5,6-*cis* product **24**.<sup>52</sup> Though there is a turnover in selectivity about the 2,6-position between the (*E*)- and (*Z*)-crotylsilanes, the reagents remain completely complementary in their stereochemical outcome. With ample quantities of all eight stereochemical analogues of 2,5,6-dihydropyrans in hand, we were positioned to complete the synthesis of each of the desired isomers of the C1–C13 portion of bistramide A.

Each dihydropyran stereoisomer was taken through an eight-step sequence to access the diastereomeric C1–C13 fragments **6** (Scheme 7). Catalytic hydrogenation with Adam's catalyst concomitantly reduced the double bonds and deprotected the benzyl ethers. The resulting alcohols were protected as TBDPS ethers, and the methyl esters were reduced with LiBH<sub>4</sub>. The newly generated alcohols were treated with (PhO)<sub>3</sub>P<sup>+</sup>CH<sub>3</sub>I<sup>-</sup> to afford primary iodides **25**. The primary iodides were displaced with the lithium anion of 2-(1-propenyl)-1,3-dithiane to give **26** as masked α,β-unsaturated systems.<sup>53</sup> The dithiane intermediates **26** were unveiled to give ketones **27** by using a mild method developed by Panek employing Dess–Martin periodinane for the oxidative removal of thioacetals.<sup>54</sup> Removal of the TBDPS ether was accomplished with wet HF in acetonitrile and oxidation of the resulting alcohols to carboxylic acids **6** occurred with catalytic chromium in wet acetonitrile. Completion of the eight stereoisomers of the C1–C13 tetrahydropyran

(50) It has been suggested that silicon prefers an axial orientation for both electronic and steric reasons but may still eliminate even without optimal overlap. For a detailed discussion and relevant examples see: Lambert, J. B. *Tetrahedron* **1990**, *46*, 2677.

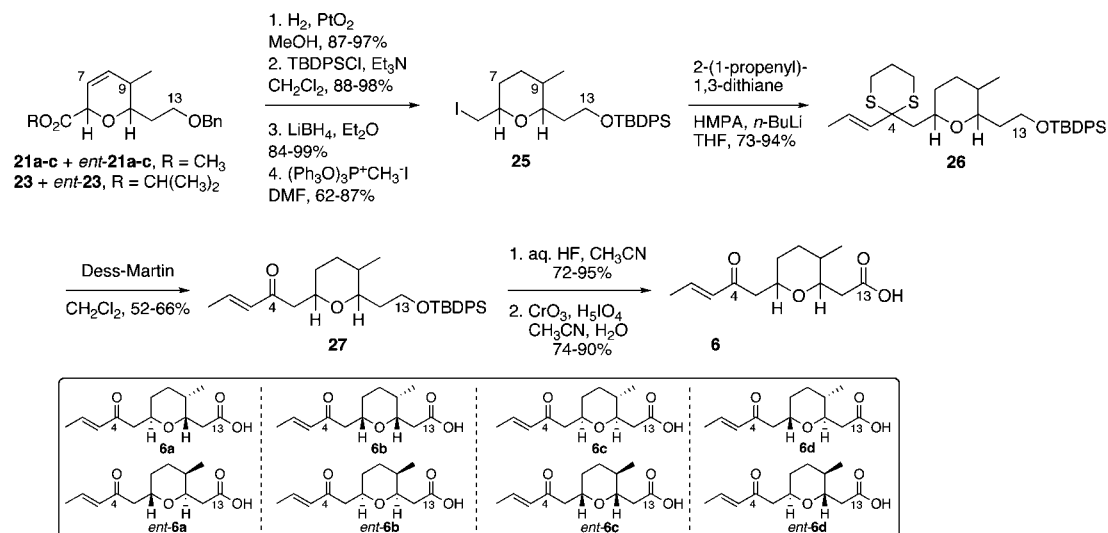
(51) Intramolecular silyl-modified Sakurai condensations of vinylsilanes suggest allylic strain plays a role in stereochemical outcome: Markó, I. E.; Dobbs, A. P.; Scheirrmann, V.; Chellé, F.; Bayston, D. J. *Tetrahedron Lett.* **1997**, *38*, 2899.

(52) It is conceivable that an *oxonia*-Cope rearrangement could play a role in the stereochemical outcome of these reactions; however, no byproducts from this pathway were observed. For an example of *oxonia*-Cope rearrangements in allyl systems, see: Roush, W. R.; Dilley, G. J. *Synlett* **2001**, 955.

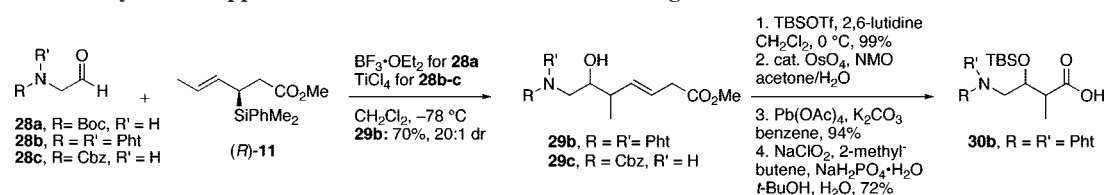
(53) (a) Corey, E. J.; Seebach, D. *Angew. Chem., Int. Ed.* **1965**, *4*, 1075. (b) Gröbel, B. T.; Seebach, D. *Synthesis* **1977**, 357.

(54) Langille, N. F.; Dakin, L. A.; Panek, J. S. *Org. Lett.* **2003**, *5*, 575.

## SCHEME 7. Synthesis of Eight Stereoisomers of the C1–C13 Tetrahydropyran Fragment 6



## SCHEME 8. Initial Synthetic Approach to the C14–C18 Amino Acid Fragment 7



fragment was accomplished in a nine-step synthetic sequence to provide the desired tetrahydropyran isomers in 20–30% overall yield.

**Synthesis of C14–C18 Subunits 7.** Our initial strategy for the preparation of C14–C18 fragments of bistramide analogues exploited a crotylation reaction between protected glycine aldehyde **28** and organosilane reagent (*R*)-**11** (Scheme 8). The newly formed homoallylic alcohols **29** were thought to be attainable with *syn* and *anti* relationships about the newly formed bond. This “turnover” in diastereoselectivity depends on the nature of Lewis acid (monodentate vs bidentate) and the presence of a heteroatom on the aldehyde capable of providing a second contact point with a Lewis acid. The latter was showcased in the synthesis of mycalolide A where the C8–C9 *anti*-configuration was obtained through chelation controlled addition of silane (*S*)-**11** with an  $\alpha$ -nitrogen bearing aldehyde.<sup>55</sup> Functionalization of the resulting alcohols **29** via a four-step sequence would afford the desired protected amino acids **30** in only five steps.

The crotylation reaction was first explored by using *tert*-butyl carbamate (Boc) protected aldehyde **28a**. Exposure of this volatile and unstable aldehyde to our standard crotylation conditions ( $\text{BF}_3 \cdot \text{OEt}_2$ ,  $\text{CH}_2\text{Cl}_2$ ) resulted in decomposition of both starting materials, including protodesilylation of crotylsilane reagent (*R*)-**11**. We next turned to condensation of phthalimide protected amino aldehyde **28b** with the organosilane reagent (*R*)-**11** in the presence of  $\text{TiCl}_4$ . The desired homoallylic alcohol **29b** was obtained in 70% yield and high diastereoselectivity (dr 20:1). This alcohol was then protected as a TBS ether and the double bond was oxidized to afford the amino acid fragment **30b** in just three steps (68% yield). Unfortunately, only the *syn*-homoallylic alcohols were observed with aldehyde **28b** when

both monodentate and bidentate Lewis acids were utilized.<sup>56</sup> Since the *anti*-C15–C16 stereochemistry was needed as well, an alternate protecting group was required that would be capable of providing a sufficiently active site for chelation. To that end, reaction of the Cbz-protected aldehyde **28c** with silane (*R*)-**11** afforded the desired alcohol **29c**, albeit in low yield and selectivity (30% yield, dr 2:1). Modification of reaction conditions (solvents, temperatures, Lewis acids) failed to improve the selectivity and yield of this reaction. Thus, we turned our efforts toward preparation of all stereoisomers of the C14–C18 amino fragment utilizing an  $\alpha$ -alkoxy aldehyde. In this case, a benzyl ether protecting group was employed to provide a second chelation site with a bidentate Lewis acid.<sup>57</sup>

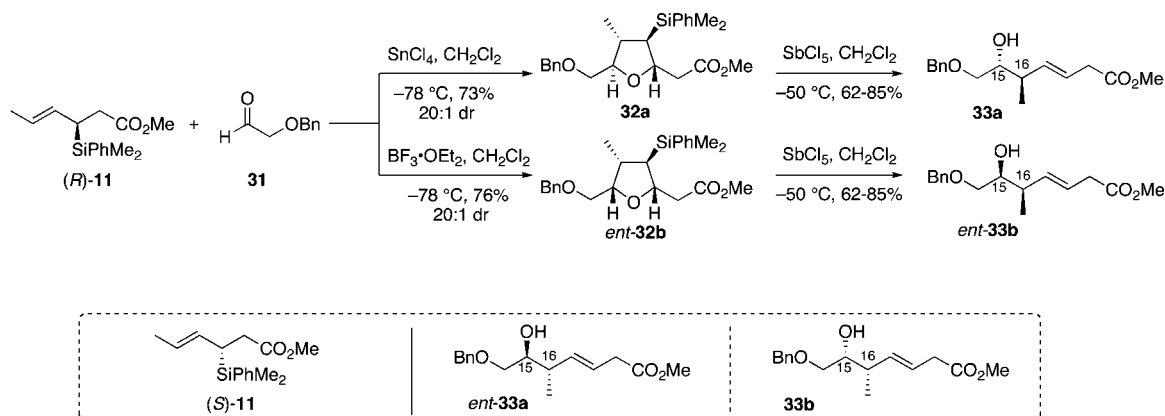
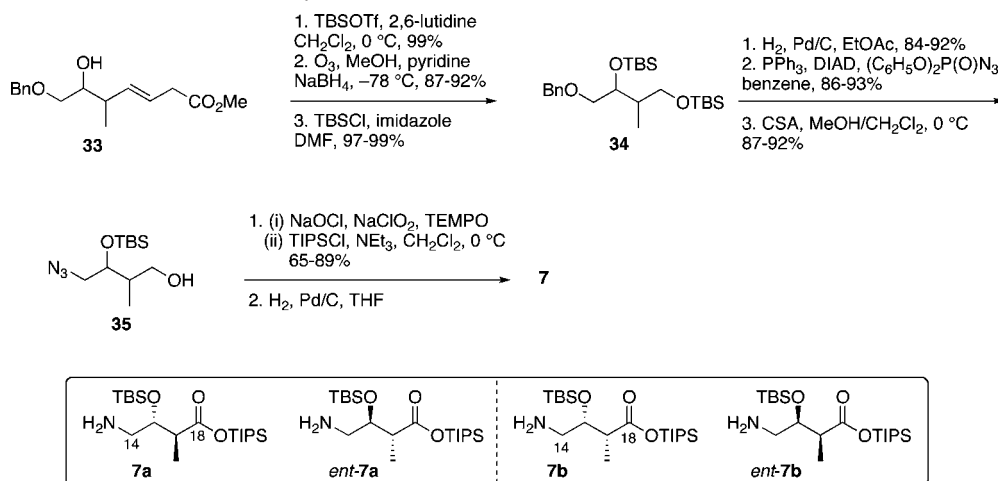
The desired *syn* and *anti* homoallylic alcohols **33** were accessed via a two-step sequence: [3+2]-annulation followed by furan opening reactions (Scheme 9).<sup>26a</sup> Use of the protected acetaldehyde **31** allowed for generation of all possible isomers of the amino acid fragment, where the primary alcohol would later be exchanged for the desired amine functionality. Condensation of (*R*)-**11** with  $\alpha$ -benzyloxyacetaldehyde **31** in the presence of  $\text{SnCl}_4$  provided 2,5-*anti*-tetrahydrofuran **32a** in 73% yield and excellent diastereoselectivity (>20:1). Use of  $\text{BF}_3 \cdot \text{OEt}_2$  as the Lewis acid promoter, on the other hand, effected formation of 2,5-*cis*-tetrahydrofuran *ent*-**32b** in 76% yield and 20:1 selectivity. These furans were then subjected to  $\text{E}_2$ -type elimination mediated by  $\text{SbCl}_5$ . The newly emerged homoallylic alcohols, **33a** and *ent*-**33b**, respectively, were obtained in moderate to good yields, 62–85%, and greater than 10 g quantities. The remaining two isomers, alcohols *ent*-**33a**

(56) The homoallylic substrates were converted to 1,1-dimethyl acetonides in a three-step sequence.

(57) (a) Panek, J. S.; Yang, M. *J. Am. Chem. Soc.* **1991**, *113*, 9868. (b) Panek, J. S.; Beres, R. *J. Org. Chem.* **1993**, *58*, 809.

(55) Liu, P.; Panek, J. S. *J. Am. Chem. Soc.* **2000**, *122*, 1235.



SCHEME 9. Preparation of C15-Homoallylic Alcohols **33**SCHEME 10. Synthesis of Four Isomers of  $\gamma$ -Amino Acid Subunit **7**

and **33b**, were also obtained in this fashion following the same reaction pathway utilizing enantiomeric crotylsilane **(S)-11**.

Completion of the synthesis of all isomers of the  $\gamma$ -amino acid fragment **7** is depicted in Scheme 10. Protection of the C15-homoallylic alcohols **33** as silyl ethers was followed by an ozonolysis/ $\text{NaBH}_4$  reduction sequence to yield primary alcohols in good yields (87–92%, 2 steps). Subsequent protection of the primary alcohols as TBS-ethers afforded the desired intermediates **34** in high yields. Cleavage of benzyl ethers (Pd/C,  $\text{H}_2$ ) gave primary alcohols which were subjected to Mitsunobu conditions by using  $(\text{PhO})_2\text{P(O)N}_3$  to install primary azides in high yields (86–93% yields). Selective removal of the primary TBS ether was effected by using CSA to provide alcohol products **35** in 87–92% yields. The required TIPS esters of the C14–C18 subunit were prepared in moderate yields via a TEMPO-mediated oxidation and protection sequence (65–89%). Reduction of the azide functionality (Pd/C,  $\text{H}_2$ ) gave the fully functionalized isomers of the amino acid fragment **7** in 15–41% yield over 10 steps.

Preparation of the left-hand side of bistramide A analogues proceeded as anticipated (Table 2). Union of eight isomers of the C1–C13 pyran fragment **6** with the four diastereomers of the  $\gamma$ -amino acid segments **7** was achieved in good yield by using the coupling reagent PyBOP in the presence of triethylamine. The TIPS-ester fragments **36** were obtained in yields ranging between 53% and 81%. It is important to note that there appears to be no stereochemical dependence on the extent of conversion and the overall yield of the coupling reactions for

either the pyran or the amino acid fragments. Each isomeric fragment **36** was prepared in greater than 40 mg quantities and showed little decomposition after prolonged storage at low temperature.

**Preparation of the Spiroketal Moiety 8.** Construction of the C29–C40 segment of the spiroketal subunit utilized starting materials obtained from a chiral pool source (Scheme 11). Subjection of the commercially available *(S)*-1,2,4-butanetriol derivative **37**<sup>58</sup> to a Wittig olefination reaction with phosphonium salt **38**<sup>59</sup> provided olefin **39** as a mixture of geometric isomers in 70% yield (*Z:E* = 10:1). The exocyclic olefin was reduced and concomitant deprotection of the benzyl ether with Raney nickel yielded a primary alcohol in 78% yield. Swern oxidation of this material provided an aldehyde, which was directly converted to the  $\alpha,\beta$ -unsaturated ketone **40** by using the Horner–Emmons reagent, diethyl 1-methyl-2-oxopropyl phosphonate.<sup>60</sup> The afforded ketone was enantioselectively reduced with Corey’s oxazaborolidine reagent [*(R)*-CBS]<sup>61</sup> to afford the *(S)*-alcohol, which was protected as a TBS ether **41** in 77% yield (2 steps). Reductive opening of the PMP acetal **41** with Dibal-H generated a secondary PMB ether in 98% yield. Conversion of this material to the triphenyl phosphine salt **42**

(58) Blakemore, P. R.; Kim, S. K.; Schulze, V. K.; White, J. D.; Yokochi, A. F. T. *J. Chem. Soc., Perkin Trans.* **2001**, *1*, 1831.

(59) Gaeta, F. C. A.; Lehman de Gaeta, L. S.; Kogan, T. P.; Or, Y. S.; Foster, C.; Czarniecki, M. *J. Med. Chem.* **1990**, *33*, 964.

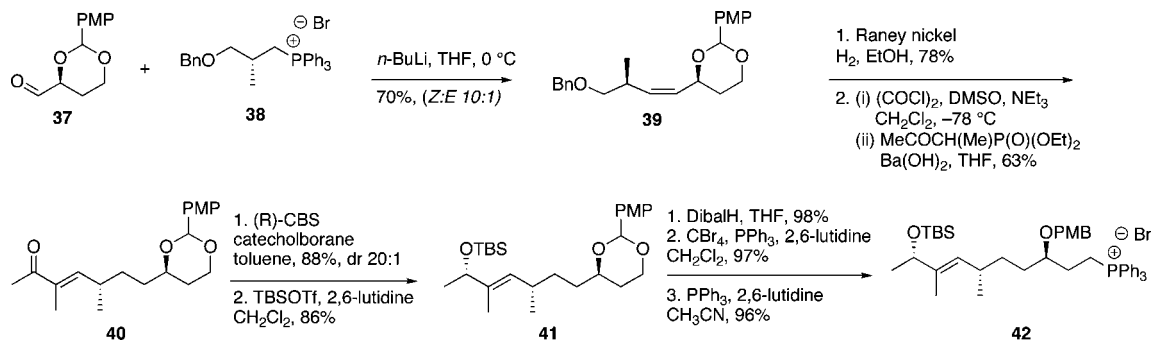
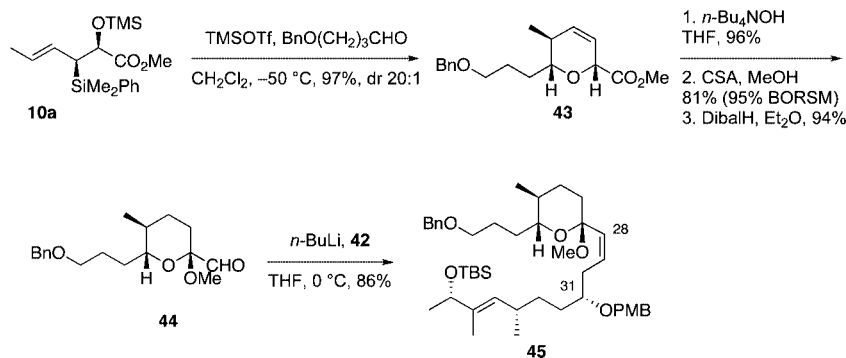
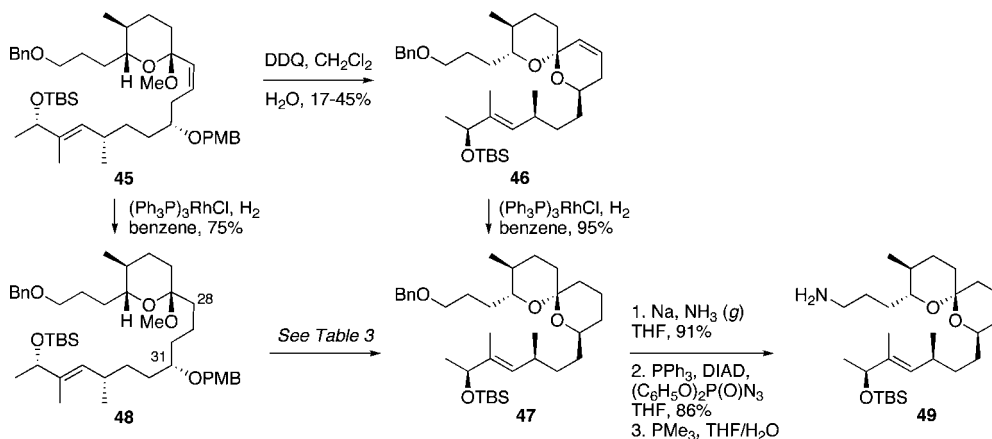
(60) Altenbach, H. J.; Korff, R. *Tetrahedron Lett.* **1981**, *22*, 5175.

(61) Corey, E. J.; Helal, C. J. *Angew. Chem., Int. Ed.* **1998**, *37*, 1986, and references found therein.

TABLE 2. Structures of C1–C18 Isomeric Fragments 36

Coupling partners	Product	Yield <sup>a</sup>	Coupling partners	Product	Yield <sup>a</sup>
6a	7a 	68	6c	7a 	64
"	ent-7a 	61	"	ent-7a 	68
"	7b 	57	"	7b 	75
"	ent-7b 	63	"	ent-7b 	68
ent-6a	7a 	61	ent-6c	7a 	71
"	ent-7a 	60	"	ent-7a 	58
"	7b 	68	"	7b 	53
"	ent-7b 	64	"	ent-7b 	59
6b	7a 	71	6d	7a 	56
"	ent-7a 	81	"	ent-7a 	59
"	7b 	69	"	7b 	66
"	ent-7b 	78	"	ent-7b 	56
ent-6b	7a 	74	ent-6d	7a 	65
"	ent-7a 	64	"	ent-7a 	64
"	7b 	80	"	7b 	74
"	ent-7b 	75	"	ent-7b 	54

<sup>a</sup> Isolated yields after SiO<sub>2</sub> column chromatography.

SCHEME 11. Reaction Sequence for the Synthesis of Phosphine Salt **42**SCHEME 12. Coupling of Tetrahydropyran **44** with the Phosphine Salt **42**SCHEME 13. Synthesis of C19–C40 Spiroketal Fragment **49**

was carried out through a standard two-step sequence: bromination of the primary alcohol was followed by displacement with PPh<sub>3</sub> to afford the advanced phosphine salt partner **42**.

Synthesis of the spiroketal portion of C19–C40 fragment **45** was initiated with a [4+2]-annulation employing *syn*-(*E*)-crotylsilane reagent **10a** and 4-(benzyloxy)butanal (Scheme 12).<sup>62</sup> The desired 2,6-*cis*-dihydropyran **43** was obtained in 97% isolated yield and high diastereoselectivity (dr 20:1). The pyran double bond was isomerized into conjugation with tetra-*n*-butyl ammonium hydroxide and subsequent treatment with methanolic CSA afforded the methyl glycoside (78% over 2 steps). This material was then reduced with Dibal-H to provide the intermediate aldehyde **44**, which was subjected to a Wittig olefination with phosphonium salt **42**. Gratifyingly, phosphorus-based olefination provided the PMB-protected (*Z*)-alkene **45** in 86% yield and as a single geometric isomer. Incorporation of a

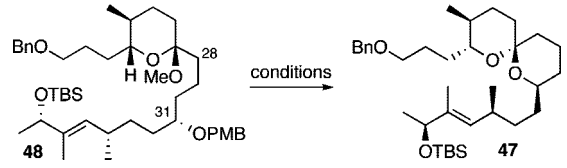
fully functionalized C40–C32 side chain prior to spirocyclization underscores the highly convergent nature of our synthesis.

Our initial approach for spirocycle formation exploited a two-step sequence: deprotection of the C31-PMB group of the C28–C29 unsaturated analogue **45** followed by spirocyclization (Scheme 13).<sup>63</sup> Unmasking the alcohol, however, proved to be very difficult as deprotection under standard DDQ conditions (CH<sub>2</sub>Cl<sub>2</sub>/H<sub>2</sub>O) did not provide the free C31-secondary alcohol as hoped, but instead gave a complex mixture of compounds. Interestingly, the major product identified from this reaction was spirocycle **46**, isolated in 17% yield after purification (Scheme 13).<sup>64</sup> Attempts to optimize the spirocyclization led to 45% yield of the desired spiroketal intermediate **46**.<sup>65</sup> Selective hydrogenation of **46** with Wilkinson's catalyst gave the required spirocycle

(63) Fénézou, J. P.; Gauchet-Prunet, J.; Julia, M.; Pancrazi, A. *Tetrahedron Lett.* **1988**, 29, 3667.

(64) For a previous example of spirocyclization in the presence of DDQ see: Paterson, I.; Chen, D. Y.-K.; Franklin, A. S. *Org. Lett.* **2002**, 4, 391.

(62) Cloarec, J.-M.; Charette, A. B. *Org. Lett.* **2004**, 6, 4731.

**TABLE 3.** Spiroketal Formation with the Saturated Framework 48


entry	conditions <sup>a</sup>	yield <sup>b</sup>
1	3 equiv of DDQ, CH <sub>2</sub> Cl <sub>2</sub> /H <sub>2</sub> O (10/1)	21
2	3 equiv of DDQ, CH <sub>2</sub> Cl <sub>2</sub> /pH 7.0 buffer	23
3	3 equiv of DDQ, CH <sub>2</sub> Cl <sub>2</sub>	<5
4	2 equiv of DDQ, CH <sub>2</sub> Cl <sub>2</sub> , 6 equiv pyridine	76
5	2 equiv of DDQ, CH <sub>2</sub> Cl <sub>2</sub> , 6 equiv pyridine	44 <sup>c</sup>

<sup>a</sup> Reactions were carried out at 0 °C. <sup>b</sup> Isolated yields after SiO<sub>2</sub> column chromatography. <sup>c</sup> Reaction was warmed to room temperature.

**47** in 95% yield. However, the low yield obtained in spirocyclization prompted us to investigate alternative conditions for this transformation.

To optimize the yield of the spirocyclization by using DDQ, the C28–C29 olefin was reduced as it may promote premature oxonium ion formation. Selective hydrogenation of the C28–C29 olefin with Wilkinson's catalyst provided the monounsaturated system **48** in 75% yield. Exposure of the C28–C29 dihydro framework **48** to DDQ under aqueous or anhydrous conditions provided low yields of the desired spiroketal **47** (entries 1–3, Table 3). However, exposure of the intermediate **48** to DDQ in the presence of pyridine under anhydrous conditions provided the desired spirocycle **47** in 76% yield (entry 4).<sup>66</sup> Warming the reaction mixture to room temperature caused significant erosion in chemical yield (entry 5). Other conditions screened for PMB deprotection/spiroketal formation include the following: TMSI,<sup>67</sup> I<sub>2</sub> in MeOH,<sup>68</sup> BCl<sub>3</sub>·Me<sub>2</sub>S complex,<sup>69</sup> and MgBr<sub>2</sub>·Et<sub>2</sub>O.<sup>70</sup>

The role of pyridine in the reaction was not explored in detail but it may behave as a simple buffer for any adventitious acid that might cause premature formation of oxonium ion.<sup>71</sup> Mechanistically, DDQ behaves as an electron acceptor to the local PMB group to form a charge transfer complex. Upon dissociation of this complex, the hydroquinone species 2,3-dichloro-5,6-dicyano-1,4-dihydroxybenzene (DDQH<sub>2</sub>) is generated. The DDQH<sub>2</sub> molecule is somewhat acidic (pK<sub>a</sub> = ~5) and was considered to be the potential cause of premature oxonium ion generation under traditional conditions (water/dichloromethane).<sup>72</sup> An additional mechanistic role of pyridine may involve production of an intermediate charge-transfer complex between pyridine and DDQ.<sup>73</sup> Charge-transfer complexes have been documented with electron-rich nitrogen heterocycles including pyrimidines and imidazoles.<sup>74</sup>

Having the desired spiroketal **47** in hand, a three-step sequence was required for completion of the C19–C40 fragment (Scheme 13). Birch reduction of the primary benzyl ether was followed by a Mitsunobu displacement of the resulting alcohol with (C<sub>6</sub>H<sub>5</sub>O)<sub>2</sub>P(O)N<sub>3</sub>. The desired primary azide was formed in 86% yield and subjected to Me<sub>3</sub>P to yield a free amine **49** via in situ hydrolysis of the phosphine imine intermediate.<sup>75</sup>

With the fully functionalized spiroketal **49** in hand, we were poised to begin construction of the complete carbon frameworks of stereochemical analogues. Accordingly, union of deprotected C1–C18 fragments **36i–l** with the spirocycle **49** was accomplished by using the PyBOP peptide coupling reagent (Scheme 14). The resulting silyl protected analogues were obtained in 41–84% yield. Applying the previously reported TBS-deprotection conditions (PPTS, MeOH) to these stereochemical derivatives proved difficult. Significant decomposition of a subset of analogues **50.16–50.24** was observed. Closer examination of the crude reaction profile suggested that the C1–C4- $\alpha,\beta$ -unsaturated system of the isomers was affected.<sup>76</sup> Removal of the C15- and C39-silyl ethers with HF, HF·pyridine, CSA, or TBAF was unsuccessful. Interestingly, use of TBAF in THF selectively removed the C15-TBS ether without decomposition of the product. With this key observation, slight modification of the spirocycle **49** was performed prior to coupling allowing access to stereochemical analogues without incident. With that accomplished, azide **51** was treated with CSA in methanol to expose alcohol (*S*)-**8** in 85% yield (Scheme 15). Reduction of azide (*S*)-**8** to the primary amine with trimethylphosphine afforded the natural spiroketal fragment (*S*)-**52**. Enantioselective inversion of the allylic alcohol intermediate (*S*)-**8** provided an additional point of stereochemical induction. The C39-hydroxyl group has been shown to have a bridged contact point with a water molecule of the Tyr143 residue of actin; this residue is also hydrogen bonded to the C18 amide of the natural product. Inversion of the C39-stereocenter was achieved in a two-step process. Oxidation of the alcohol (*S*)-**8** with Dess–Martin periodinane afforded an  $\alpha,\beta$ -unsaturated ketone (92% yield), which was reduced with (*S*)-CBS reagent to give the C39-epimeric alcohol (*R*)-**8** in good yield and diastereoselectivity (81%, dr 20:1). Staudinger reaction and hydrolysis of the resulting iminophosphorane provided the unnatural spiroketal fragment (*R*)-**52**, epimeric at C39.

Completion of the skeletal backbones of stereochemical analogues was achieved in two steps (Scheme 16). Coupling of C1–C18 acids **36a–p** and *ent*-**36a–p** with the natural spiroketal (*S*)-**52** was mediated with PyBOP after initial treatment of TIPS-acids with TBAF. The resulting C15-protected alcohol products **53.1–53.32** were obtained in 60–80% yield. Subjectation of these advanced intermediates to TBAF afforded the bistramide A as well as the desired 31 unnatural products

(65) Anhydrous conditions resulted in no reactions while using phosphate buffer (pH 7) provided 19% yield of the desired spirocycle.

(66) Conditions found in Table 3 were also applied to **44** with little success.

(67) Gordon, D. M.; Danishefsky, S. J. *J. Am. Chem. Soc.* **1992**, *114*, 659.

(68) Vaino, A. R.; Szarek, W. A. *Synlett* **1995**, 1157.

(69) Congreve, M. S.; Davison, E. C.; Fuhry, M. A. M.; Holmes, A. B.; Payne, A. N.; Robinson, R. A.; Ward, S. E. *Synlett* **1993**, 663.

(70) Onoda, T.; Shirai, R.; Iwasaki, S. *Tetrahedron Lett.* **1997**, *38*, 1443.

(71) The use of collidine as a buffer (against DDQH<sub>2</sub>) in the DDQ oxidation of silyl enol ethers has also been noted, see: (a) Fleming, I.; Paterson, I. *Synthesis* **1979**, 736. (b) Siewert, J.; Textor, A.; Grond, S.; von Zezschwitz, P. *Chem. Eur. J.* **2007**, *13*, 7424. (c) Banwell, M. G.; Hockless, D. C. R.; McLeod, M. D. *New J. Chem.* **2003**, *27*, 50. (d) Fevig, T. L.; Elliott, R. L.; Curran, D. P. *J. Am. Chem. Soc.* **1988**, *110*, 5064.

(72) Akutagawa, T.; Saito, G. *Bull. Chem. Soc. Jpn.* **1995**, *68*, 1753.

(73) (a) Bhattacharya, A.; DiMichele, L. M.; Dolling, U. H.; Grabowski, E. J. J.; Grenda, V. J. *J. Org. Chem.* **1989**, *54*, 6118. (b) Bhattacharya, A.; DiMichele, L. M.; Dolling, U. H.; Douglas, A. W.; Grabowski, E. J. J. *J. Am. Chem. Soc.* **1988**, *110*, 3318. (c) Wallace, D. J.; Gibb, A. D.; Cottrell, I. F.; Kennedy, D. J.; Brands, K. M. J.; Dolling, U. H. *Synthesis* **2001**, *12*, 1784.

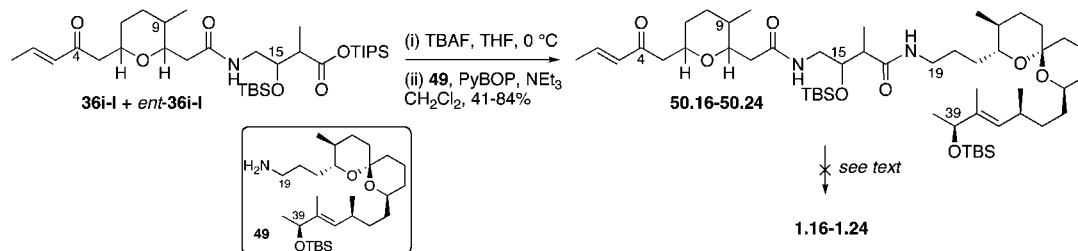
(74) Charge-transfer complexes with other nitrogen heterocycles including imidazoles and pyrimidines have been reported, see: (a) Salman, H. M. A.; Rabie, U. M.; Abd-Alla, E. M. *Can. J. Anal. Sci. Spectrosc.* **2004**, *49*, 1. (b) Boraie, A. A. A. *Spectrochim. Acta, Part A* **2002**, *58*, 1895. (c) Khashaba, P. Y.; El-Shabouri, S. R.; Emara, K. M.; Mohamed, A. M. *J. Pharm. Biomed. Anal.* **2000**, *22*, 363.

(75) For a review of the Staudinger reaction see: Gololobov, Y. G.; Kasukhin, L. F. *Tetrahedron* **1992**, *48*, 1353.

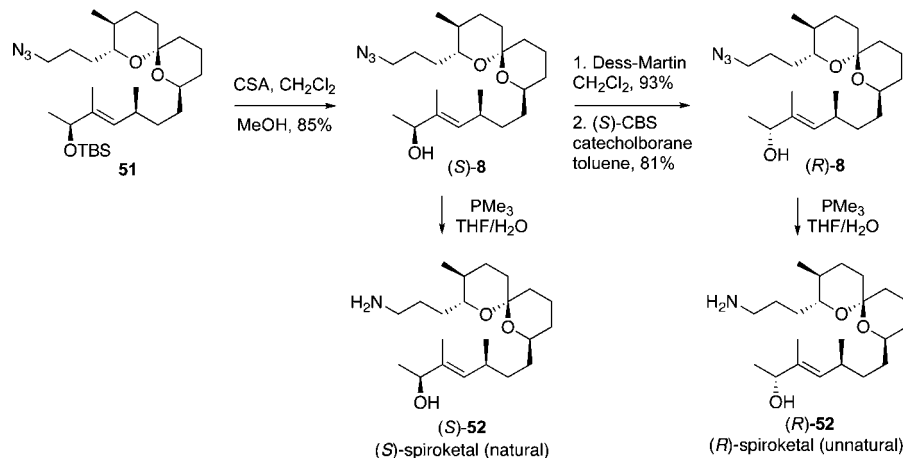
(76) The unknown product was obtained as a mixture of isomers with a loss of C2–C3 olefin. We were unable to separate the mixture for characterization.



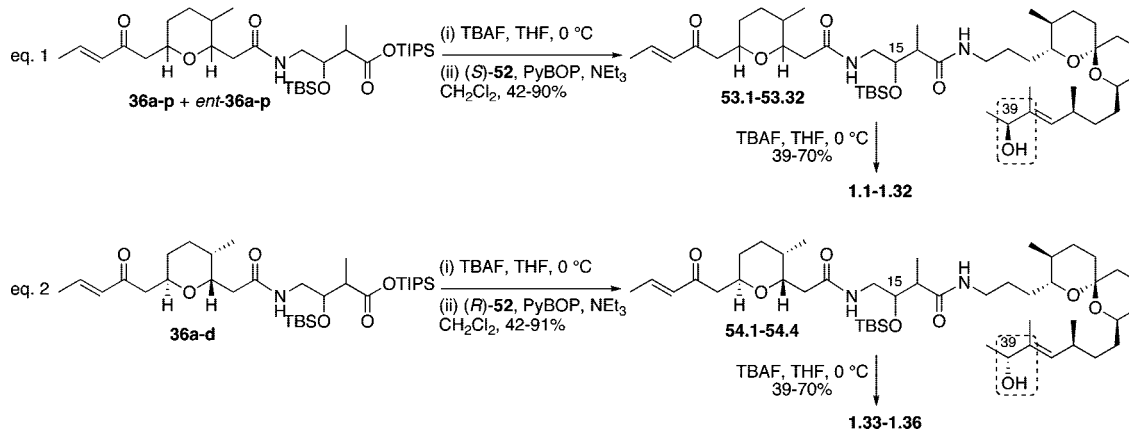
## SCHEME 14. Coupling of Acids 36 and Spiroketal 49 and Silyl Deprotection



## SCHEME 15. Preparation of the C39-Epimer of the Spiroketal Subunit 52



## SCHEME 16. Completion of the Synthesis of Stereoisomers 1.1–1.36



**1.2–1.32** in good yields and greater than 3 mg quantities. On the other hand, union of (*R*)-spiroketal **52** with the isomers of the natural pyran **36a–d** provided four additional epimers **1.33–1.36** of the natural product.

**Biological Evaluation of Bistramide A Stereochemical Analogues.** The 35-membered stereochemical library of bistramide A was screened for cytotoxicity and disruption of cellular actin. The stereostructure activity relationships (SSAR) of bistramide A **1.1** and its derivatives (**1.2–1.36**) were explored by using cell growth assays: renal carcinoma line UO-31 and the CNS tumor cell line SF-295 (Table 4). By using a 2-day assay for cell growth inhibition of UO-31 cells, analogue **1.21** was shown to be approximately twice as potent (44 nM) as the natural product **1.1** (77 nM). Interestingly, compound **1.21** differs stereochemically from bistramide A **1.1** at the C6 and C9 positions of the pyran moiety (Figure 2). The C1–C13 portion of the bistramide A is not involved in polar contacts with the protein but was suggested to only attenuate lipophilicity

of the natural product in the barbed end binding pocket. A recent publication describes computational docking studies using the X-ray structure concerning the structural determinants of macrolide–actin binding.<sup>14</sup> In this study, flexible docking of the bistramide A pyran fragment in the hydrophobic cleft of actin revealed at least three hydrophobic interactions between the protein and tetrahydropyran/enone portion of the molecule. The highest scoring flexibly docked structure was thus shown to have rotation around the C12–C13 bond of the natural product. Thus, the results of the computational docking experiments may help to explain the enhanced activity of analogue **1.21** in the UO-31 cell line.

Six other epimers demonstrated submicromolar potency against the UO-31 cell line (Table 4). Similar to the **1.21** variant, the derivatives **1.5**, **1.9**, **1.17**, **1.25**, and **1.29** differ only in stereochemistry at the C6, C9, and C11 positions of the pyran moiety (Figure 2). Interestingly, compound **1.33**, the C39-epimer of the natural product, also showed good micromolar potency.

**TABLE 4.** Cell-Growth Inhibition of Bistramide Stereochemical Analogues 1.1–1.36 Against UO-31 and SF-295 Cancer Cell Lines

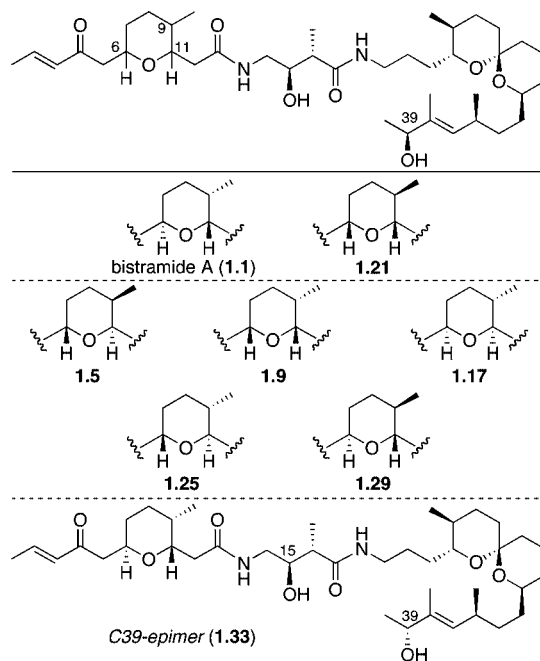
compound	UO-31 (IC <sub>50</sub> ± SEM μM)	SF-295 (IC <sub>50</sub> ± SEM μM)
1.1	0.071 ± 0.01	0.47 ± 0.2
1.2	5.9 ± 1.1	– <sup>a</sup>
1.3	45 ± 8	78.8 ± 4
1.4	4.6 ± 0.7	4.7 ± 2
1.5	0.62 ± 0.03	2 ± 0
1.6	14.8 ± 4.5	– <sup>a</sup>
1.7	45.3 ± 0.5	76.5
1.8	15.9 ± 7.3	– <sup>a</sup>
1.9	0.32 ± 0.02	0.2 ± 0.0
1.10	15.6 ± 4.5	– <sup>a</sup>
1.11	17.1 ± 2.2	– <sup>a</sup>
1.12	2.8 ± 0.4	– <sup>a</sup>
1.13	1.9 ± 0.2	~2.4 <sup>b</sup>
1.14	7.8 ± 3.5	77.5 ± 4
1.15	18.2 ± 5.8	– <sup>a</sup>
1.16	11 ± 1.4	~96 <sup>b</sup>
1.17	0.33 ± 0.02	3.5
1.18	13.9 ± 5.3	– <sup>a</sup>
1.19	44.7 ± 9.7	– <sup>a</sup>
1.20	14.5 ± 5	~14 <sup>b</sup>
1.21	0.044 ± 0.017	~3.8 <sup>b</sup>
1.22	44.7 ± 20.7	– <sup>a</sup>
1.23	6.2 ± 0.5	17.1 ± 6
1.24	45.1 ± 30.8	75.2
1.25	5.7 ± 0.7	~34 <sup>b</sup>
1.26	0.82 ± 0.07	~30 <sup>b</sup>
1.27	17.4 ± 6.4	– <sup>a</sup>
1.28	15 ± 9.9	– <sup>a</sup>
1.29	0.81 ± 0.08	~20 <sup>b</sup>
1.30	14.9 ± 0.4	– <sup>a</sup>
1.31	14.6 ± 10.2	– <sup>a</sup>
1.32	5.3 ± 1.4	– <sup>a</sup>
1.33	0.33 ± 0.04	0.34 ± 0.1
1.34	12 ± 1.7	– <sup>a</sup>
1.35	15.4 ± 9.3	– <sup>a</sup>
1.36	2.2 ± 0.3	~16 <sup>b</sup>

<sup>a</sup> Compounds were not tested. <sup>b</sup> Estimated IC<sub>50</sub> value.

The remainder of the stereoisomers exhibited lower activity for the UO-31 cell line, with the least potent analogue **1.7** having an IC<sub>50</sub> value of 45.3 μM (Table 4).

A subset of the compounds was also tested against the CNS tumor cell line SF-295 under the same protocol (Table 4). In general, the compounds inhibited cell growth to a lesser degree, but the relative rank potency was similar to the UO-31 cell line. Stereoisomer **1.33** showed a slightly better inhibition (0.34 μM) in comparison to bistramide A (0.47 μM) for the SF-295 cell line.

The effects on cell cycle were assessed for two of the most potent cell growth inhibiting compounds (**1.1** and **1.33**), as well as for the least active one (**1.7**). A dose responsive reduction of the proportion of cells in S phase and increase in G1 phase by analogues **1.1** and **1.33** was observed. These effects were demonstrated in both the UO-31 and SF-295 cell lines indicating blockade of the cell cycle by the two isomers. Stereoisomer **1.7**, which was essentially inactive as an inhibitor of cell growth, also had no effect on the cell cycle. As such, cell cycle data are presented for a relatively potent library member, the natural product (bistramide A), as well as a very weak binding member of the collection. The essential point is that potent members of the library appear to block the cell cycle in a manner consistent with actin inhibition, while weak members of the collection do not.

**FIGURE 2.** Representative structures of potent stereochemical analogues of Bistramide A.**TABLE 5.** Pearson Correlation Coefficients between Compounds 1.1 and 1.21 and Other Known actin-Binding Natural Products<sup>a</sup>

name	NSC	GI <sub>50</sub> to 1.1	GI <sub>50</sub> to 1.21
aplyronine A	687160	–0.11	–0.03
cytochalasin A	174119	0.55	0.42
cytochalasin B	107658	0.55	0.49
cytochalasin D	209835	0.71	0.63
cytochalasin E	175151	0.71	0.66
cytochalasin H	305222	0.69	0.56
cytochalasin Q	675858	0.69	0.49
dolastatin 11	606195	0.37	0.45
jasplakinolide	613009	0.34	0.41
latrunculin A	613011	0.58	0.44
mycalolide C, D mixture	V4827	0.28	0.50
mycalolide E	V4828	0.30	0.50
swinholid H	685570	0.49	0.61

<sup>a</sup> Correlations were obtained for the GI<sub>50</sub> level of response.

The inhibition of cell cycle by bistramide A **1.1** and analogue **1.33** was confirmed with confocal microscopy examination of FITC-phalloidin stained cells. At concentrations that inhibited cell growth and cell cycle progression, the actin cytoskeleton was disrupted as indicated by the loss of fluorescence and alteration of the cytoskeletal structure. These effects were consistent with both cell lines.

Finally, the natural product **1.1** and C6,C9-stereochemical analogue **1.21** were subjected to the NCI 60-cell assay. The obtained results provide further insight into the action of bistramide A and its epimers. Stereoisomer **1.21** was approximately twice as potent as the natural product **1.1**, with mean GI<sub>50</sub> values of 9 and 18 nM, respectively. The patterns of cell growth inhibition were highly correlated (Pearson coefficient of 0.81 at the GI<sub>50</sub> level and 0.81 at the TGI level of response). The most sensitive panels were the renal cancer cell lines and the CNS cancer cell lines. The difference between the least and most sensitive cell lines was between 2 and 2.5 log units at the GI<sub>50</sub> level of response, and approximately 3.5 log units at the TGI level. These data were compared to that of other compounds known to bind to and

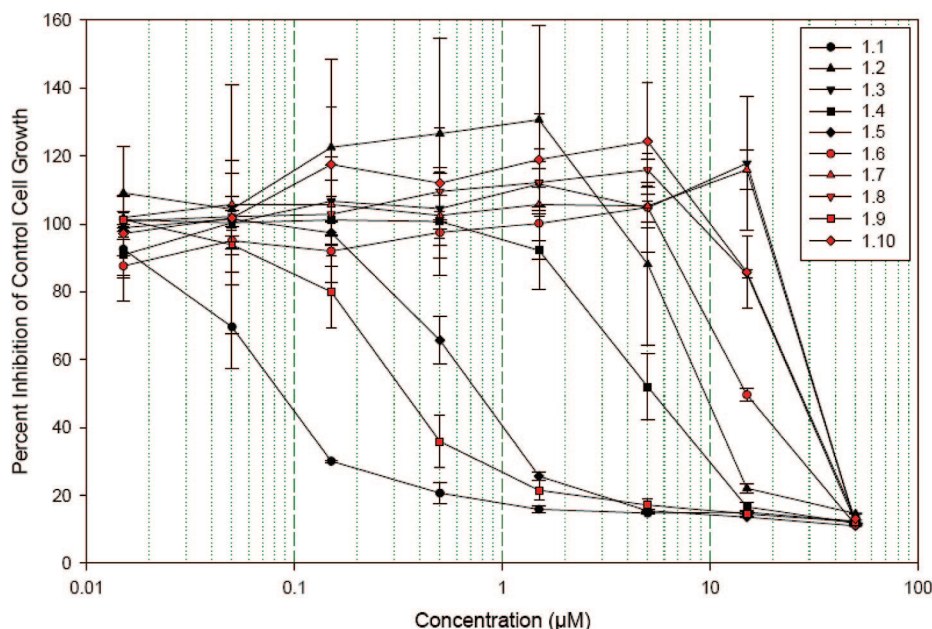


FIGURE 3. Cell-growth inhibition of stereochemical analogues 1.1–1.10 against renal carcinoma cell line UO-31.

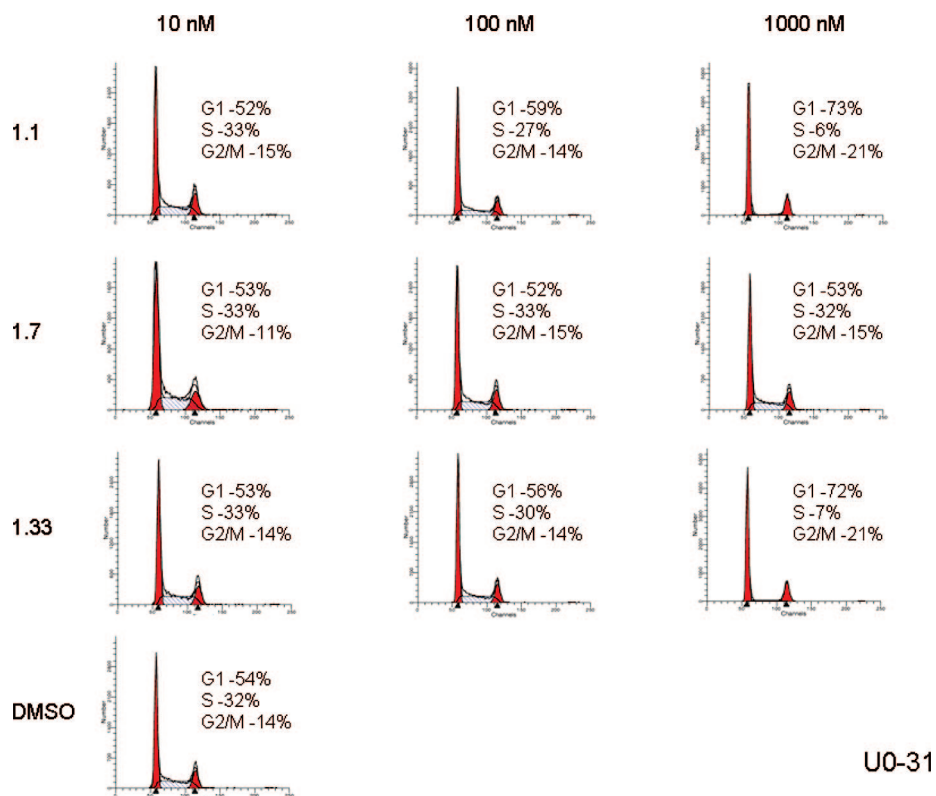


FIGURE 4. Cell cycle analysis of the UO-31 cell line for the most potent cell growth inhibiting isomers 1.1 and 1.33 and least active isomer 1.7.

interfere with actin (Table 5). With the notable exception of aplyronine A, the data for all other natural products showed significant, albeit modest, correlations in 60-cell patterns to the data for compounds 1.1 and 1.21.

**Biological Activity: Experimental. Cytotoxicity Assays.** A tetrazolium dye [2,3-bis(2-methoxy-4-nitro-5-sulphophenyl)-2H-tetrazolium-5-carboxanilide; XTT]-based colorimetric assay was used in 96-well plates to measure inhibition of the

proliferation/survival of tumor cell lines in vitro (Figure 3).<sup>77</sup> All test compounds were formulated in DMSO and applied to cells such that the final DMSO concentration was  $\leq 0.1\%$ .

**Cell Cycle Analysis.** SF-295 and UO-31 cells were harvested from flasks at 75–85% confluency, counted, and plated into

(77) Scudiero, D. A.; Shoemaker, R. H.; Paull, K. D.; Monks, A.; Tierney, S.; Nofziger, T. H.; Currens, M. J.; Seniff, D.; Boyd, M. R. *Cancer Res.* **1988**, *48*, 4827.

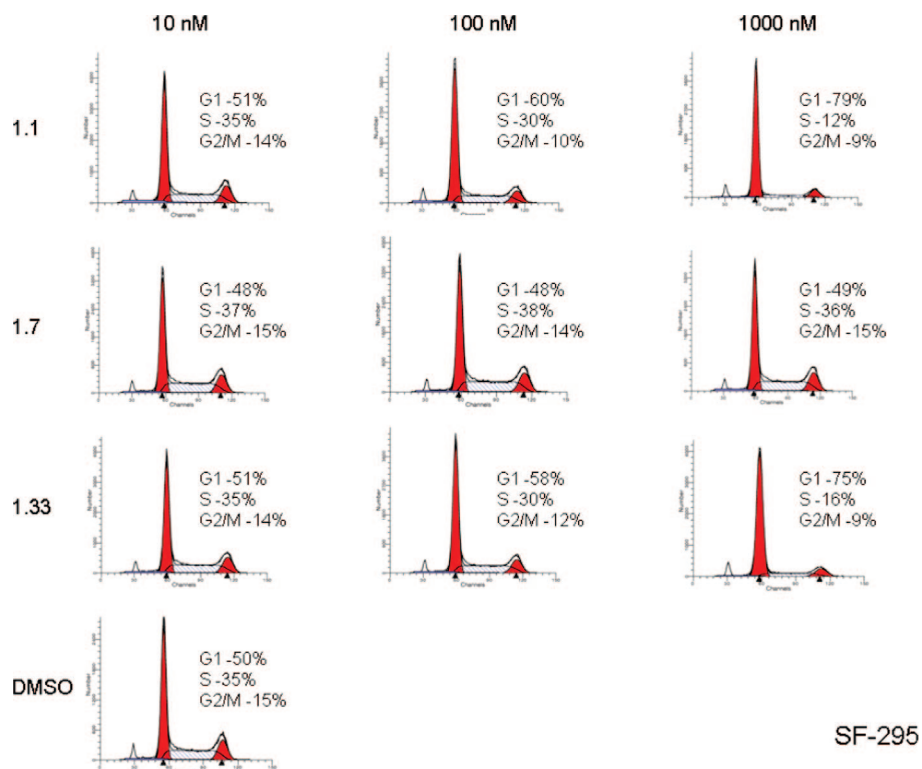


**FIGURE 5.** Cell cycle analysis of the SF-295 cell line for the most potent cell growth inhibiting analogues **1.1** and **1.33** and least active stereochemical compound **1.7**.

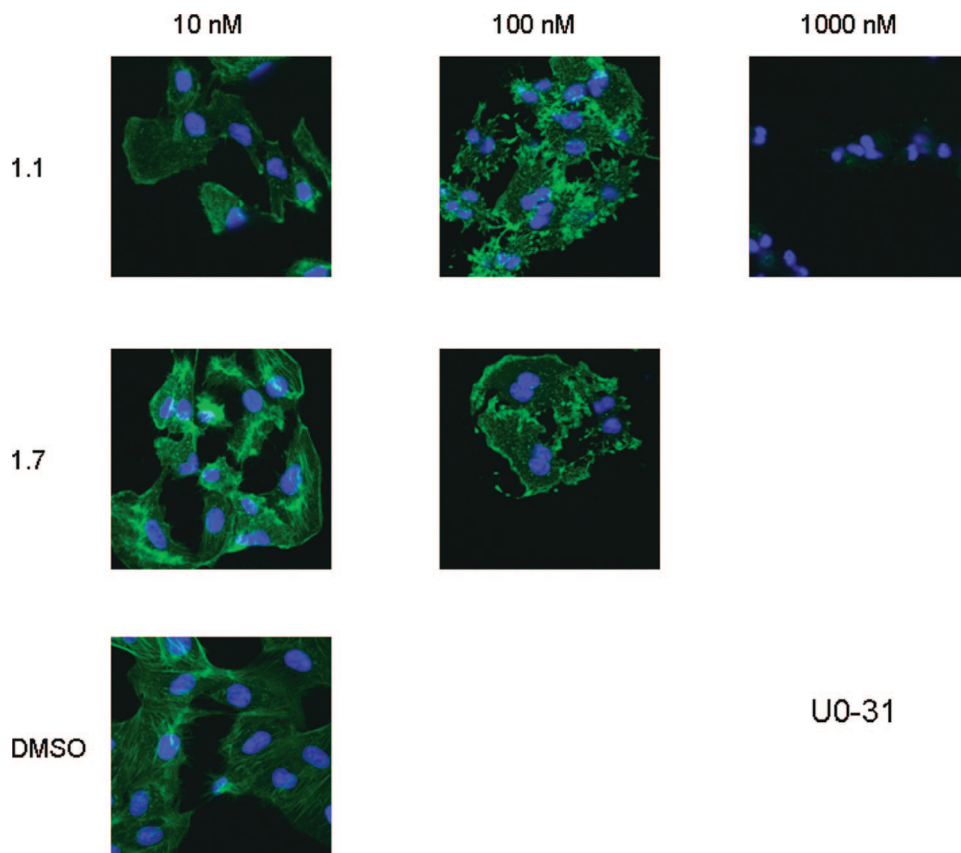


**FIGURE 6.** Confocal microscopy using phalloidin staining images of UO-31 cells. Bistramide **1.1** causes disruption of the F-actin in a dose dependent manner, while the least active epimer **1.7** does not.

35-mm dishes at a density of approximately  $1 \times 10^6$  cells/dish, then allowed to reattach overnight. Compounds were prepared

as a 5 mM stock solution in DMSO and applied to cells at final concentrations of 1, 0.1, and 0.001  $\mu$ M. A control dish was



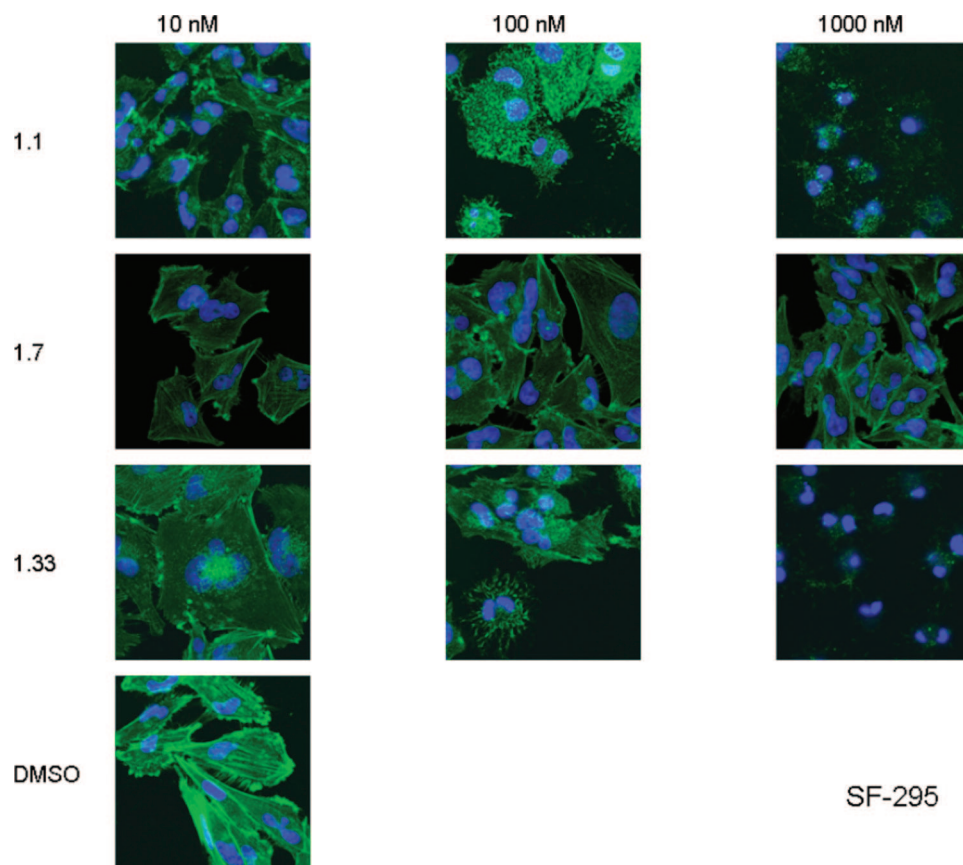


**FIGURE 7.** Confocal microscopy using phalloidin staining images of SF-295 cells. Bistramide **1.1** and its stereochemical analogue **1.33** cause disruption of the F-actin in dose dependent manner, while the least active epimer **1.7** does not.

treated with vehicle (DMSO) alone. Cells were incubated for 24 h in the continuous presence of the various treatments, at which times they were rinsed with PBS, harvested by trypsinization, resuspended in complete medium, pelleted by centrifugation, rinsed once with PBS, and resuspended in 1 mL of Krishan's buffer (0.1% sodium citrate, 0.02 mg/mL RNase, 0.3% NP-40 and 50 mg/mL of propidium iodide (PI) at pH 7.4). Cells were analyzed for relative DNA content by flow cytometry by using a Becton Dickinson FACScan (Becton Dickinson Immunocytometry Systems, San Jose, CA) equipped with a DDM using CELLQuest software. The analysis was done with MODFIT LT 2.0 (Verity Software House, Inc., Topsham, ME).

**Confocal Images.** UO-31 and SF-295 cell monolayers were established on glass coverslips and incubated overnight with the compounds (Figures 4–7). After treatment, the cells were fixed in 3.7% formaldehyde, permeabilized with 0.1% Triton X-100, and stained with fluorescein phalloidin (Molecular Probes, Invitrogen Corporation, Carlsbad, CA) at a final concentration of 165 nM. After staining, slides were rinsed with PBS, and mounted in a DAPI containing mounting medium (Molecular Probes). Confocal images were acquired using a 63 $\times$  oil objective (Zeiss UV510, Oberkochen, Germany).

**NCI 60-Cell Assay.** The NCI 60-cell assay was conducted as previously described.<sup>78</sup> Compounds were tested first at a single  $10^{-5}$  M dose, then at two separate times in full dose response format in five 10-fold dilutions. Comparison analyses were performed as previously described.<sup>79</sup>

## Conclusions

We have shown that by employing a unified strategy, the creation of a library of selected stereoisomers of the natural product bistramide A is viable, providing the reaction methodology is sufficiently robust. We have learned that the generation of unique biological information on stereostructure–activity relationships (SSAR) is a consequence of such an approach. In the present case, we have sampled a small number of stereoisomers (35 of the 2048 possible compounds), selected where crystallographic studies have indicated that the chirality might be critical for binding to actin. Our synthetic strategy was highlighted by preparation of the stereochemical variants of the principle fragments with three structurally and stereochemically different enantioenriched organosilane reagents. The compounds were screened for growth inhibition against UO-31 and SF-295 cell lines as well as for binding to actin. Six stereoisomers (**1.5**, **1.9**, **1.17**, **1.29**, and **1.33**) inhibited growth in the micromolar range, while compound **1.21** was shown to be the most potent in the UO-31 cell line assay. Stereochemical analogue **1.21** was shown to be approximately twice as potent as the natural bistramide A **1.1** with mean  $GI_{50}$  values of 9 and 18 nM, respectively, in the NCI 60 cell assay. Given that stereoisomer libraries are generally difficult to achieve by solution phase synthesis is a testament to the versatility of chiral silane-based bond construction methodology. Enabling enhanced facility in asymmetric synthesis and more efficient

(78) Monks, A.; Scudiero, D. A.; Johnson, G. S.; Paull, K. D.; Sausville, E. A. *Anti-Cancer Drug Des.* **1997**, *12*, 533.

(79) Paull, K. D.; Shoemaker, R. H.; Hodes, L.; Monks, A.; Scudiero, D. A.; Rubinstein, L.; Plowman, J.; Boyd, M. R. *J. Natl. Cancer Inst.* **1989**, *81*, 1088.

modular tactics in convergent assembly make it possible to elucidate the role of each chiral center in bioactivity. With bistramide A, the correlation to crystallographic data validated the approach, but it should be possible to empirically probe stereochemical factors in the absence of a target as well. For compounds with large numbers of chiral centers, it may not be desirable to synthesize all possible stereoisomers, but an iterative approach which samples several centers in each stage to guide successive syntheses should facilitate a complete analysis of SSAR, when coupled with high throughput biological testing methods.

## Experimental Section

The following experimental information is representative and describe the complete details of the convergent synthesis of bistramide A stereoisomer **1.21**.

**(2S,5R,6S)-Methyl 6-(2-(Benzyloxy)ethyl)-5-methyl-5,6-dihydro-2H-pyran-2-carboxylate (ent-21c)**. To a solution of 3-(benzyloxy)propanal **20** (1.87 g, 11.4 mmol) and (*E*)-*syn* crotylsilane *ent-10a* (2.00 g, 5.70 mmol) in methylene chloride (120 mL) at  $-50\text{ }^{\circ}\text{C}$  was added trimethylsilyl trifluoromethanesulfonate (2.08 mL, 11.4 mmol) dropwise. The reaction was stirred for 24 h at  $-50\text{ }^{\circ}\text{C}$  before it was quenched with saturated  $\text{NaHCO}_3$  and warmed to room temperature. The layers were separated and the aqueous layer was extracted with methylene chloride (3 $\times$ ). The combined organic layers were dried with magnesium sulfate, filtered, and concentrated under reduced pressure. Purification by column chromatography (silica, 10% EtOAc/hexanes) afforded dihydropyran *ent-21c* in 72% yield.  $[\alpha]_D^{25} -116.7$  (*c* 2.0,  $\text{CHCl}_3$ );  $^1\text{H NMR}$  ( $\text{CDCl}_3$ , 400 MHz)  $\delta$  7.33–7.25 (m, 5H), 5.73 (tq, *J* = 2.0, 10.2, 22.6 Hz, 2H), 4.67 (m, 1H), 4.50 (q, *J* = 12.0, 24.0 Hz, 1H), 3.75 (s, 3H), 3.72–3.61 (m, 2H), 3.32 (dt, *J* = 2.4, 9.6 Hz, 1H), 2.21 (m, 1H), 2.08–2.00 (m, 1H), 1.84–1.75 (m, 1H), 0.93 (d, *J* = 7.2 Hz, 3H);  $^{13}\text{C NMR}$  ( $\text{CDCl}_3$ , 100 MHz)  $\delta$  170.6, 138.6, 134.0, 128.3, 127.6, 127.4, 133.3, 77.3, 74.7, 72.9, 66.7, 52.3, 34.0, 33.2, 17.1; IR (neat)  $\nu_{\text{max}}$  2958, 2870, 1736, 1263, 1097, 700  $\text{cm}^{-1}$ ; HRMS (CI,  $\text{NH}_3$ ) *m/z* calcd for  $\text{C}_{17}\text{H}_{22}\text{O}_4$  [*M* + 23] $^+$  313.1416, found 313.1354.

**(2S,5R,6S)-Methyl 6-(2-Hydroxyethyl)-5-methyltetrahydro-2H-pyran-2-carboxylate**. To a solution of pyran *ent-21c* (0.880 g, 3.01 mmol) in methanol (19 mL) was added  $\text{PtO}_2$  (0.171 g, 25 mol %). The reaction flask was then placed under an atmosphere of hydrogen and stirred for 12 h. The heterogeneous mixture was filtered over Celite, washed with methanol, and concentrated in vacuo. Purification by flash chromatography (silica, 50% EtOAc/hexanes) provided 95% of the desired product as a clear oil.  $[\alpha]_D^{25} -60.1$  (*c* 1.0,  $\text{CHCl}_3$ );  $^1\text{H NMR}$  ( $\text{CDCl}_3$ , 400 MHz)  $\delta$  3.94 (dd, *J* = 2.6, 11.8 Hz, 1H), 3.76 (m, 2H), 3.69 (s, 3H), 3.21 (dt, *J* = 2.8, 9.8 Hz, 1H), 1.97–1.80 (m, 3H), 1.73 (m, 1H), 1.55 (dq, *J* = 3.8, 13.0, 25.0 Hz, 1H), 1.43 (m, 1H), 1.22 (dt, *J* = 3.8, 13.0, 25.2 Hz, 1H), 0.79 (d, *J* = 6.4 Hz, 3H);  $^{13}\text{C NMR}$  ( $\text{CDCl}_3$ , 100 MHz)  $\delta$  171.5, 84.7, 76.1, 61.3, 52.0, 34.7, 34.6, 32.0, 28.8, 17.3; IR (neat)  $\nu_{\text{max}}$  3460, 2954, 2929, 2876, 1753, 1439, 1212, 1088  $\text{cm}^{-1}$ ; HRMS (CI,  $\text{NH}_3$ ) *m/z* calcd for  $\text{C}_{10}\text{H}_{19}\text{O}_4$  [*M* + 1] $^+$  203.1283, found 203.1286.

**(2S,5R,6S)-Methyl 6-(2-(tert-Butyldiphenylsilyloxy)ethyl)-5-methyltetrahydro-2H-pyran-2-carboxylate**. To a solution of alcohol (2.90 g, 14.3 mmol) in *N,N*-dimethylformamide (22.0 mL) at  $0\text{ }^{\circ}\text{C}$  was added 1*H*-imidazole (1.20 g, 17.9 mmol) followed by *tert*-butylchlorodiphenylsilane (4.10 mL, 15.8 mmol) dropwise. The reaction was allowed to warm to room temperature on its own and was stirred for 16 h at room temperature. The reaction mixture was then diluted with water and extracted with  $\text{Et}_2\text{O}$  (3 $\times$ ). The combined organic layers were dried with magnesium sulfate, filtered, and concentrated under reduced pressure. Purification by flash chromatography (silica, 3% EtOAc/hexanes) provided 99% of the desired product as a clear oil.  $[\alpha]_D^{25} -34.1$  (*c* 2.0,  $\text{CHCl}_3$ );

$^1\text{H NMR}$  ( $\text{CDCl}_3$ , 400 MHz)  $\delta$  7.64 (m, 4H), 7.36 (m, 5H), 3.91 (dt, *J* = 4.8, 9.6 Hz, 1H), 3.84 (dd, *J* = 2.2, 11.8, 1H), 3.76 (m, 1H), 3.72 (s, 3H), 3.17 (dt, *J* = 2.2, 9.4 Hz, 1H), 2.00–1.81 (m, 3H), 1.67–1.53 (m, 2H), 1.40 (m, 1H), 1.23 (m, 1H), 1.02 (s, 9H), 0.81 (d, *J* = 6.4 Hz, 3H);  $^{13}\text{C NMR}$  ( $\text{CDCl}_3$ , 100 MHz)  $\delta$  172.1, 135.56, 135.55, 134.1, 134.0, 129.47, 129.44, 127.55, 127.53, 80.2, 60.0, 51.9, 35.7, 34.6, 32.7, 29.4, 26.9, 19.2, 17.7; IR (neat)  $\nu_{\text{max}}$  2955, 2930, 2856, 1428, 1112, 702  $\text{cm}^{-1}$ ; HRMS (CI,  $\text{NH}_3$ ) *m/z* calcd for  $\text{C}_{26}\text{H}_{36}\text{O}_4\text{Si}$  [*M*] $^+$  440.2383, found 440.2334.

**(2S,5R,6S)-6-(2-(tert-Butyldiphenylsilyloxy)ethyl)-5-methyltetrahydro-2H-pyran-2-yl)methanol**. To a solution of ester (1.24 g, 28.1 mmol) in diethyl ether (25.0 mL) at  $0\text{ }^{\circ}\text{C}$  was added lithium tetrahydroborate (1.23 g, 5.60 mmol) in one portion. The reaction mixture was allowed to warm to room temperature and stirred for an additional 2 h. The reaction was then quenched by addition of water and the solution was stirred until bubbling ceased. Layers were separated and the aqueous layer was extracted with  $\text{Et}_2\text{O}$  (3 $\times$ ). The combined organic layers were dried with magnesium sulfate, filtered, and concentrated under reduced pressure. Purification by flash chromatography (silica, 10% EtOAc/hexanes) provided 88% of the desired product as a clear oil.  $[\alpha]_D^{25} -26.0$  (*c* 1.1,  $\text{CHCl}_3$ );  $^1\text{H NMR}$  ( $\text{CDCl}_3$ , 400 MHz)  $\delta$  7.66 (m, 4H), 7.38 (m, 6H), 3.78 (m, 2H), 3.50 (dt, *J* = 3.0, 8.8 Hz, 1H), 3.43–3.30 (m, 2H), 3.12 (dt, *J* = 2.0, 9.6 Hz, 1H), 1.96 (m, 1H), 1.78 (m, 2H), 1.54 (m, 1H), 1.45 (m, 1H), 1.34–1.11 (m, 2H), 1.03 (s, 9H), 0.80 (d, *J* = 6.8 Hz, 3H);  $^{13}\text{C NMR}$  ( $\text{CDCl}_3$ , 75 MHz)  $\delta$  135.5, 134.0, 129.5, 127.6, 79.8, 77.5, 66.3, 60.3, 36.1, 35.1, 32.4, 27.6, 26.9, 19.2, 17.7; IR (neat)  $\nu_{\text{max}}$  3448, 3069, 2931, 2858, 1428, 1102, 703  $\text{cm}^{-1}$ ; HRMS (CI,  $\text{NH}_3$ ) *m/z* calcd for  $\text{C}_{25}\text{H}_{38}\text{O}_3\text{Si}$  [*M* + 23] $^+$  414.2593, found 414.2560.

**tert-Butyl(2-((2S,3R,6S)-6-(iodomethyl)-3-methyltetrahydro-2H-pyran-2-yl)ethoxy)diphenylsilane (ent-25c)**. To a solution of alcohol (3.60 g, 8.72 mmol) and 2,6-lutidine (2.38 mL, 20.6 mmol) in *N,N*-dimethylformamide (70.0 mL) at  $0\text{ }^{\circ}\text{C}$  was added methyltriphenoxyphosphonium iodide (8.48 g, 18.8 mmol) in one portion. The reaction was stirred for 1 h at  $0\text{ }^{\circ}\text{C}$  before diethyl ether and water were added. Layers were separated and the aqueous layer was extracted with diethyl ether (3 $\times$ ). The combined organic layers were dried with magnesium sulfate, filtered, and concentrated under reduced pressure. Purification by flash chromatography (silica, 3% EtOAc/hexanes) provided *ent-25c* in 79% as a clear oil.  $[\alpha]_D^{25} -3.9$  (*c* 1.5,  $\text{CHCl}_3$ );  $^1\text{H NMR}$  ( $\text{CDCl}_3$ , 400 MHz)  $\delta$  7.66 (m, 4H), 7.35 (m, 5H), 3.85 (m, 2H), 3.23 (m, 1H), 3.12 (dt, *J* = 2.0, 9.6 Hz, 1H), 3.05 (d, *J* = 5.6 Hz, 2H), 1.95 (m, 1H), 1.83–1.74 (m, 2H), 1.53 (m, 2H), 1.30–1.16 (m, 2H), 1.04 (s, 9H), 0.80 (d, *J* = 6.8 Hz, 3H);  $^{13}\text{C NMR}$  ( $\text{CDCl}_3$ , 75 MHz)  $\delta$  135.8, 134.4, 129.7, 127.8, 80.6, 77.7, 60.6, 36.3, 35.0, 32.9, 31.9, 27.2, 19.5, 17.7, 10.0; IR (neat)  $\nu_{\text{max}}$  3068, 2931, 2857, 1465, 1097, 702  $\text{cm}^{-1}$ ; HRMS (CI,  $\text{NH}_3$ ) *m/z* calcd for  $\text{C}_{25}\text{H}_{35}\text{IO}_2\text{Si}$  [*M* + 23] $^+$  545.1349, found 545.1363.

**tert-Butyl(2-((2S,3R,6S)-3-methyl-6-((*E*)-prop-1-enyl)-1,3-dithian-2-yl)methyl)tetrahydro-2H-pyran-2-yl)ethoxy)diphenylsilane (ent-26c)**. To a solution of 2-((*E*)-1-propenyl)-[1,3]-dithiane (2.02 g, 12.6 mmol) and hexamethylphosphoramide (3.30 mL, 18.9 mmol) in tetrahydrofuran (50.0 mL) at  $-78\text{ }^{\circ}\text{C}$  was added *tert*-butyllithium in pentane (1.70 M, 7.43 mL) dropwise. The reaction mixture was stirred for 1 h at  $-78\text{ }^{\circ}\text{C}$  before a solution of iodide *ent-25c* (3.30 g, 6.32 mmol) in tetrahydrofuran (50.0 mL) was added dropwise. The reaction mixture was then allowed to stir for 1 h at  $-78\text{ }^{\circ}\text{C}$ , warmed to  $0\text{ }^{\circ}\text{C}$ , and stirred for an additional hour. Reaction was quenched by addition of water and extracted with diethyl ether (3 $\times$ ). The combined organic layers were dried with magnesium sulfate, filtered, and concentrated under reduced pressure. Purification by flash chromatography (silica, 1% EtOAc/hexanes) provided *ent-26c* in 90% as a clear oil.  $[\alpha]_D^{25} -7.9$  (*c* 2.5,  $\text{CHCl}_3$ );  $^1\text{H NMR}$  ( $\text{CDCl}_3$ , 400 MHz)  $\delta$  7.65 (m, 4H), 7.37 (m, 6H), 5.80 (m, 1H), 5.43 (d, *J* = 15.2 Hz, 1H), 3.83 (m, 2H), 3.38 (m, 1H), 2.99 (dt, *J* = 2.0, 9.6 Hz, 1H), 2.76 (m, 1H), 2.67–2.56 (m, 3H), 2.09 (dd, *J* = 6.8, 14.8 Hz, 1H), 1.91–1.75

(m, 4H), 1.70 (m, 1H), 1.64 (d,  $J = 6.4$  Hz, 3H), 1.55 (m, 2H), 1.35–1.13 (m, 3H), 1.02 (s, 9H), 0.76 (d,  $J = 6.4$  Hz, 3H);  $^{13}\text{C}$  NMR ( $\text{CDCl}_3$ , 75 MHz)  $\delta$  135.6, 134.3, 133.7, 129.4, 128.4, 127.5, 80.4, 74.3, 61.4, 53.1, 48.1, 36.3, 34.8, 33.2, 33.1, 27.1, 27.0, 26.9, 25.2, 19.2, 17.8, 17.5; IR (neat)  $\nu_{\text{max}}$  3068, 2928, 2856, 1428, 1087, 703  $\text{cm}^{-1}$ ; HRMS (CI,  $\text{NH}_3$ )  $m/z$  calcd for  $\text{C}_{32}\text{H}_{46}\text{O}_2\text{Si}$  [ $\text{M} + 554.2708$ , found 554.2720.

**(E)-1-((2S,5R,6S)-6-(2-(tert-Butyldiphenylsilyloxy)ethyl)-5-methyltetrahydro-2H-pyran-2-yl)pent-3-en-2-one (ent-27c).** To a solution of dithiane *ent-26c* (100 mg, 0.180 mmol) in a mixture of acetonitrile (4.00 mL), methylene chloride (0.500 mL), and water (0.500 mL) was added Dess–Martin periodinane in methylene chloride (0.30 M, 1.20 mL) dropwise. The reaction was allowed to stir at room temperature for 5 h before ethyl acetate and water were added. Layers were separated and water was extracted with ethyl acetate (3 $\times$ ). The combined organic layers were dried with magnesium sulfate, filtered, and concentrated under reduced pressure. Purification by flash chromatography (silica, 2–5% EtOAc/hexanes) provided *ent-27c* in 60% as a clear oil.  $[\alpha]_{\text{D}}^{25}$   $-22.7$  ( $c$  1.1,  $\text{CHCl}_3$ );  $^1\text{H}$  NMR ( $\text{CDCl}_3$ , 400 MHz)  $\delta$  7.64 (m, 4H), 7.34 (m, 6H), 6.76 (m, 1H), 6.07 (d,  $J = 15.6$  Hz, 1H), 3.79–3.63 (m, 3H), 3.09 (dt,  $J = 1.6, 9.2$  Hz, 1H), 2.71 (A of ABX,  $J = 6.0, 14.8$  Hz, 1H), 2.46 (B of ABX,  $J = 6.0, 15.2$  Hz, 1H), 1.91 (m, 1H), 1.79 (d,  $J = 6.8$  Hz, 3H), 1.74–1.63 (m, 2H), 1.50 (m, 1H), 1.22 (m, 3H), 1.02 (s, 9H), 0.78 (d,  $J = 6.0$  Hz, 3H);  $^{13}\text{C}$  NMR ( $\text{CDCl}_3$ , 75 MHz)  $\delta$  198.7, 143.0, 135.5, 134.1, 132.5, 129.4, 127.5, 80.2, 74.3, 60.4, 46.6, 36.2, 35.0, 32.8, 32.2, 29.7, 26.9, 19.2, 18.2; IR (neat)  $\nu_{\text{max}}$  3068, 2954, 2857, 1672, 1632, 1431, 1108, 703  $\text{cm}^{-1}$ ; HRMS (CI,  $\text{NH}_3$ )  $m/z$  calcd for  $\text{C}_{29}\text{H}_{40}\text{O}_3\text{Si}$  [ $\text{M} + 23$ ] $^+$  487.2644, found 487.2681.

**(E)-1-((2S,5R,6S)-6-(2-Hydroxyethyl)-5-methyltetrahydro-2H-pyran-2-yl)pent-3-en-2-one.** To a solution of *ent-27c* (100 mg, 0.215 mmol) in a nalgene vial in acetonitrile (10.0 mL) at room temperature was added hydrofluoric acid (1.00 mL) dropwise. The reaction was allowed to stir for 3 h at room temperature before it was quenched by slow addition of saturated  $\text{NaHCO}_3$ . The aqueous layer was extracted with ethyl acetate (3 $\times$ ). The combined organic layers were dried with magnesium sulfate, filtered, and concentrated under reduced pressure. Purification by flash chromatography (silica, 50% EtOAc/hexanes) provided product in 95% as a clear oil.  $[\alpha]_{\text{D}}^{25}$   $-25.3^\circ$  ( $c$  2.9,  $\text{CHCl}_3$ );  $^1\text{H}$  NMR ( $\text{CDCl}_3$ , 400 MHz)  $\delta$  6.85 (dq,  $J = 6.8, 13.6$  Hz, 1H), 6.11 (ddd,  $J = 1.6, 3.2, 15.8$  Hz, 2H), 3.81 (m, 1H), 3.71 (dt,  $J = 1.6, 4.4$  Hz, 2H), 3.20 (dt,  $J = 2.8, 9.6$  Hz, 1H), 2.79 (A of ABX,  $J = 8.0, 15.6$  Hz, 1H), 2.51 (B of ABX,  $J = 4.8, 15.6$  Hz, 1H), 1.88 (dd,  $J = 1.8, 7.0$  Hz, 3H), 1.84 (m, 1H), 1.76 (dq,  $J = 2.8, 6.8$  Hz, 1H), 1.66–1.52 (m, 2H), 1.40–1.17 (m, 3H), 0.79 (d,  $J = 6.8$  Hz, 3H);  $^{13}\text{C}$  NMR ( $\text{CDCl}_3$ , 100 MHz)  $\delta$  198.3, 143.6, 132.5, 84.6, 74.3, 61.5, 46.0, 35.0, 34.7, 32.5, 31.8, 18.3, 17.6; IR (neat)  $\nu_{\text{max}}$  3447, 2924, 2873, 1670, 1631, 1441, 1085, 973  $\text{cm}^{-1}$ ; HRMS (CI,  $\text{NH}_3$ )  $m/z$  calcd for  $\text{C}_{13}\text{H}_{23}\text{O}_3$  [ $\text{M} + 1$ ] $^+$  227.1647, found 227.1670.

**2-((2S,3R,6S)-3-Methyl-6-((E)-2-oxopent-3-enyl)tetrahydro-2H-pyran-2-yl)ethanoic Acid (ent-6c).** To a solution of alcohol (45.0 mg, 0.199 mmol) in acetonitrile (1 mL), and water (15  $\mu\text{L}$ ) at 0  $^\circ\text{C}$  was added  $\text{CrO}_3/\text{H}_5\text{IO}_6$  stock solution (500  $\mu\text{L}$ ) dropwise. The reaction was stirred at 0  $^\circ\text{C}$  for 0.5 h before another equivalent of  $\text{CrO}_3/\text{H}_5\text{IO}_6$  stock solution (500  $\mu\text{L}$ ) was added dropwise and then the reaction was stirred for 0.5 h at 0  $^\circ\text{C}$ . The reaction was then quenched by addition of  $\text{Na}_2\text{HPO}_4$  (60 mg/1 mL of  $\text{H}_2\text{O}$ ), diluted with ethyl ether, and stirred for 30 min at room temperature. Layers were separated and the aqueous layer was extracted with ethyl ether (3 $\times$ ). Combined organic layers were dried with magnesium sulfate, filtered, and concentrated under reduced pressure. Purification by flash chromatography (silica, 50% EtOAc/hexanes) provided *ent-6c* in 80% as a clear oil.  $[\alpha]_{\text{D}}^{25}$   $-35.1$  ( $c$  1.0,  $\text{CHCl}_3$ );  $^1\text{H}$  NMR ( $\text{CDCl}_3$ , 400 MHz)  $\delta$  6.84 (dq,  $J = 7.0, 13.8, 15.6$  Hz, 1H), 6.10 (dq,  $J = 1.6, 3.2, 15.6$  Hz, 1H), 3.86 (m, 1H), 3.42 (dt,  $J = 3.0, 9.4$  Hz, 1H), 2.80 (A of ABX,  $J = 7.6, 15.6$  Hz, 1H), 2.67 (A of ABX,  $J = 2.8, 15.6$  Hz, 1H), 2.57 (B of ABX,

$J = 5.0, 15.6$  Hz, 1H), 2.38 (B of ABX,  $J = 9.6, 15.6$  Hz, 1H), 1.87 (dd,  $J = 1.6, 6.8$  Hz, 3H), 1.79 (m, 1H), 1.68 (m, 1H), 1.41–1.20 (m, 3H), 0.83 (d,  $J = 6.8$  Hz, 3H);  $^{13}\text{C}$  NMR ( $\text{CDCl}_3$ , 75 MHz)  $\delta$  198.2, 174.5, 143.8, 132.2, 79.9, 74.4, 45.9, 38.7, 34.8, 32.1, 31.6, 18.3, 17.4; IR (neat)  $\nu_{\text{max}}$  2929, 1713, 1631, 1438, 1194, 1082, 971  $\text{cm}^{-1}$ ; HRMS (CI,  $\text{NH}_3$ )  $m/z$  calcd for  $\text{C}_{13}\text{H}_{20}\text{O}_4$  [ $\text{M} + 23$ ] $^+$  263.1259, found 263.1249.

**(2S,3R)-Triisopropylsilyl 3-(tert-Butyldimethylsilyloxy)-2-methyl-4-(2-((2S,3R,6S)-3-methyl-6-((E)-2-oxopent-3-enyl)tetrahydro-2H-pyran-2-yl)ethanamido)butanoate (ent-36j).** A solution of azide (1.00 mg, 0.233 mmol) in tetrahydrofuran (10.0 mL) was treated with 10 wt % palladium on activated carbon (5.0 mg). The reaction flask was flushed with argon and hydrogen atmospheres sequentially. The reaction was then placed under an atmosphere of hydrogen and stirred for 12 h. The heterogeneous mixture was filtered over Celite, rinsed with tetrahydrofuran, and concentrated in vacuo. The resulting thick oil of **7a** was used in the next step without further purification.

To a solution of the crude amine **7a** in methylene chloride (10.0 mL) was added crude acid *ent-6c* (50.0 mg, 0.208 mmol), PyBOP (119 mg, 0.229 mmol), and triethylamine (34.8  $\mu\text{L}$ , 0.250 mmol). The reaction mixture was allowed to stir for 24 h at room temperature. Upon completion of the reaction, diethyl ether was added. The organic layer was washed sequentially with water, saturated sodium bicarbonate, and brine solutions. The combined organic layers were dried with magnesium sulfate, filtered, and concentrated under reduced pressure. Purification by flash chromatography (silica, 20% EtOAc/hexanes) provided product *ent-36j* in 71% as a clear oil.  $[\alpha]_{\text{D}}^{25}$   $-9.5$  ( $c$  1.0,  $\text{CHCl}_3$ );  $^1\text{H}$  NMR ( $\text{CDCl}_3$ , 400 MHz)  $\delta$  6.81 (m, 2H), 6.06 (dd,  $J = 1.6, 16.0$  Hz, 1H), 4.07 (q,  $J = 6.4, 10.4$  Hz, 1H), 3.79 (m, 1H), 3.48 (quint,  $J = 6.8, 13.2$  Hz, 1H), 3.29 (dt,  $J = 1.8, 9.2$  Hz, 1H), 3.17 (dt,  $J = 5.4, 13.6$  Hz, 1H), 2.77 (A of ABX,  $J = 7.0, 16.8$  Hz, 1H), 2.63 (m, 1H), 2.56 (B of ABX,  $J = 5.8, 16.8$  Hz, 1H), 2.49 (A of ABX,  $J = 2.0, 15.6$  Hz, 1H), 2.20 (B of ABX,  $J = 9.2, 15.6$  Hz, 1H), 1.84 (dd,  $J = 1.6, 6.8$  Hz, 3H), 1.73 (m, 1H), 1.62 (m, 1H), 1.24 (m, 6H), 1.13 (d,  $J = 7.6$  Hz, 3H), 1.03 (d,  $J = 7.6$  Hz, 18 H), 0.82 (s, 9H), 0.79 (d,  $J = 6.4$  Hz, 3H), 0.04 (s, 3H), 0.03 (s, 3H);  $^{13}\text{C}$  NMR ( $\text{CDCl}_3$ , 75 MHz)  $\delta$  197.6, 173.7, 171.3, 142.9, 132.1, 80.6, 73.7, 71.9, 46.1, 45.1, 42.6, 40.5, 34.6, 32.3, 31.5, 25.8, 18.2, 18.0, 17.8, 17.7, 12.8, 11.8,  $-4.5, -4.9$ ; IR (neat)  $\nu_{\text{max}}$  3361, 2932, 2867, 1674, 1464, 1194, 1085, 837  $\text{cm}^{-1}$ ; HRMS (CI,  $\text{NH}_3$ )  $m/z$  calcd for  $\text{C}_{33}\text{H}_{64}\text{O}_6\text{NSi}_2$  [ $\text{M} + 1$ ] $^+$  626.4272, found 626.4299.

**(2S,5S,E)-7-((2S,6S,8R,9S)-8-(3-Azidopropyl)-9-methyl-1,7-dioxaspiro[5.5]undecan-2-yl)-3,5-dimethylhept-3-en-2-ol ((S)-8).** To a solution of **51** (50.0 mg, 0.0986 mmol) in a mixture of methylene chloride (1.0 mL) and methanol (1.0 mL) at 0  $^\circ\text{C}$  was added 10-camphorsulfonic acid (7.0 mg, 0.03 mmol). The reaction was allowed to stir at 0  $^\circ\text{C}$  for 2 h before it was quenched with a saturated solution of  $\text{NaHCO}_3$ . The aqueous layer was extracted with dichloromethane (3 $\times$ ). The combined organic layers were dried with magnesium sulfate, filtered, and concentrated under reduced pressure. Purification by column chromatography (silica, 15% EtOAc/hexanes) affords alcohol (**S**)-**8** in 85% as a clear oil.  $[\alpha]_{\text{D}}^{25}$   $-36.9$  ( $c$  0.3,  $\text{CHCl}_3$ );  $^1\text{H}$  NMR ( $\text{CDCl}_3$ , 400 MHz)  $\delta$  5.16 (d,  $J = 9.2$  Hz, 1H), 4.17 (q,  $J = 6.0, 12.4$  Hz, 1H), 3.41 (br t, 1H), 3.30 (m, 2H), 3.14 (t,  $J = 9.6$  Hz, 1H), 2.33 (m, 1H), 1.91 (m, 1H), 1.75 (m, 2H), 1.60 (s, 3H), 1.58–1.28 (m, 15H), 1.23 (d,  $J = 6.4$  Hz, 3H), 0.91 (d,  $J = 6.8$  Hz, 3H), 0.82 (d,  $J = 6.4$  Hz, 3H);  $^{13}\text{C}$  NMR ( $\text{CDCl}_3$ , 100 MHz)  $\delta$  137.2, 131.4, 95.5, 74.1, 73.4, 69.2, 51.9, 36.0, 35.4, 35.0, 34.1, 33.6, 31.9, 31.3, 30.3, 27.9, 25.5, 21.6, 21.0, 19.2, 18.0, 11.8; IR (neat)  $\nu_{\text{max}}$  3407, 2932, 2868, 2095, 1457, 1225, 1096, 985  $\text{cm}^{-1}$ ; HRMS (CI,  $\text{NH}_3$ )  $m/z$  calcd for  $\text{C}_{22}\text{H}_{39}\text{O}_3\text{N}_3$  [ $\text{M} + 23$ ] $^+$  416.2889, found 416.2913.

**(S,E)-7-((2S,6S,8R,9S)-8-(3-Azidopropyl)-9-methyl-1,7-dioxaspiro[5.5]undecan-2-yl)-3,5-dimethylhept-3-en-2-one.** To a solution of (**S**)-**8** (38.0 mg, 0.0966 mmol) in methylene chloride (9.70 mL) at 0  $^\circ\text{C}$  was added Dess–Martin periodinane (0.552 mL, 0.35 M in methylene chloride) dropwise. The reaction was allowed



to warm to room temperature over 1 h and was diluted with ethyl acetate. The organic layer was washed with a saturated solution of sodium bicarbonate followed by sodium chloride solution. The combined organic layers were dried with magnesium sulfate, filtered, and concentrated under reduced pressure. Purification by column chromatography (silica, 10% EtOAc/hexanes) gives product as a colorless glass (35.0 mg, 0.0894 mmol, 92.5%).  $[\alpha]_D^{25} +37.8$  (*c* 0.8, CHCl<sub>3</sub>); <sup>1</sup>H NMR (CDCl<sub>3</sub>, 400 MHz)  $\delta$  6.37 (d, *J* = 9.6 Hz, 1H), 3.43 (m, 1H), 3.31 (d quint, 2H), 3.13 (dt, *J* = 2.4, 9.6 Hz, 1H), 2.55 (m, 1H), 2.30 (s, 3H), 1.92 (m, 1H), 1.80 (m, 1H), 1.76 (s, 3H), 1.71 (m, 1H), 1.62–1.44 (m, 8H), 1.36 (m, 7H), 1.13 (dq, *J* = 3.6, 12.8, 25.2 Hz, 1H), 1.03 (d, *J* = 6.8 Hz, 3H), 0.82 (d, *J* = 6.8 Hz, 3H); <sup>13</sup>C NMR (CDCl<sub>3</sub>, 100 MHz)  $\delta$  200.2, 149.2, 136.3, 95.5, 74.2, 69.0, 51.9, 36.0, 35.4, 34.9, 34.2, 33.7, 32.9, 31.3, 30.3, 27.8, 25.5, 25.4, 20.0, 19.1, 18.0, 11.4; IR (neat)  $\nu_{\max}$  2932, 2869, 2095, 1670, 1457, 1096, 986 cm<sup>-1</sup>; HRMS (CI, NH<sub>3</sub>) *m/z* calcd for C<sub>22</sub>H<sub>37</sub>O<sub>3</sub>N<sub>3</sub> [M + 23]<sup>+</sup> 414.2733, found 414.2733.

**(2R,5S,E)-7-((2S,6S,8R,9S)-8-(3-Azidopropyl)-9-methyl-1,7-dioxaspiro[5.5]undecan-2-yl)-3,5-dimethylhept-3-en-2-ol ((R)-8).** To a solution of ketone (13.0 mg, 0.0332 mmol) in toluene (2.00 mL) at -78 °C was added (*S*)-CBS (39.8  $\mu$ L, 0.0398 mmol, 1.0 M in toluene) dropwise. After 5 min, catecholborane (66.4  $\mu$ L, 0.0664 mmol, 1.0 M in toluene) was added dropwise and the reaction mixture was allowed to stir at -78 °C for 24 h. Reaction was quenched by addition of methanol (0.070 mL) and was allowed to warm to room temperature and then stirred for 1 h. The mixture was diluted with ethyl acetate and a saturated solution of sodium bicarbonate. The aqueous layer was extracted with ethyl acetate (3 $\times$ ). The combined organic layers were dried with magnesium sulfate, filtered, and concentrated under reduced pressure. Purification by column chromatography (silica, 15% EtOAc/hexanes) affords alcohol (*R*)-**8** as a colorless glass (13.0 mg, 0.0330 mmol, 99%).  $[\alpha]_D^{25} +39.6$  (*c* 0.3, CHCl<sub>3</sub>); <sup>1</sup>H NMR (CDCl<sub>3</sub>, 400 MHz)  $\delta$  5.16 (d, *J* = 9.2 Hz, 1H), 4.17 (q, *J* = 6.0, 12.4 Hz, 1H), 3.41 (br. t, 1H), 3.30 (m, 2H), 3.14 (t, *J* = 9.6 Hz, 1H), 2.33 (m, 1H), 1.91 (m, 1H), 1.75 (m, 2H), 1.60 (s, 3H), 1.58–1.28 (m, 15H), 1.23 (d, *J* = 6.4 Hz, 3H), 0.91 (d, *J* = 6.8 Hz, 3H), 0.82 (d, *J* = 6.4 Hz, 3H); <sup>13</sup>C NMR (CDCl<sub>3</sub>, 100 MHz)  $\delta$  137.2, 131.4, 95.5, 74.1, 73.4, 69.2, 51.9, 36.0, 35.4, 35.0, 34.1, 33.6, 31.9, 31.3, 30.3, 27.9, 25.5, 21.6, 21.0, 19.2, 18.0, 11.8; IR (neat)  $\nu_{\max}$  3407, 2932, 2868, 2095, 1457, 1225, 1096, 985 cm<sup>-1</sup>; HRMS (CI, NH<sub>3</sub>) *m/z* calcd for C<sub>22</sub>H<sub>39</sub>O<sub>3</sub>N<sub>3</sub> [M + 23]<sup>+</sup> 416.2889, found 416.2913.

**(2S,3R)-3-Hydroxy-N-(3-((2R,3S,6S,8S)-8-((3S,6S,E)-6-hydroxy-3,5-dimethylhept-4-enyl)-3-methyl-1,7-dioxaspiro[5.5]undecan-2-yl)propyl)-2-methyl-4-(2-((2S,3R,6S)-3-methyl-6-((E)-2-oxopent-3-enyl)tetrahydro-2H-pyran-2-yl)ethanamido)butanamide (1.21).** To a solution of azide (*S*)-**8** (5.00 mg, 0.0127 mmol) in a mixture of tetrahydrofuran (0.900 mL) and water (0.300 mL) at room temperature was added trimethyl phosphine (63.5  $\mu$ L, 1.0 M in tetrahydrofuran) dropwise. The reaction was allowed to stir for 1 h and then diluted with a saturated solution of sodium chloride. The aqueous layer was extracted with ethyl ether (3 $\times$ ). The combined organic layers were dried with magnesium sulfate, filtered, and concentrated under reduced pressure. The crude, clear oil was used directly in the coupling step without further purification.

To a solution of TIPS acid *ent*-**36j** (8.00 mg, 0.0128 mmol) in THF (1.30 mL) at 0 °C was added TBAF (14.7  $\mu$ L, 1.00 M in THF) dropwise. The reaction was stirred for 0.5 h before it was diluted with ethyl acetate. The organic layer was washed with 0.01 M HCl and brine solutions. The combined organic layers were dried

with magnesium sulfate, filtered, and concentrated under reduced pressure. The crude acid was used in the coupling step without further purification.

To a solution of C1–C18 acid and C19–C40 amine (*S*)-**52** (6.00 mg, 0.0163 mmol) in methylene chloride (1.60 mL) at room temperature was added PyBOP (9.34 mg, 0.0180 mmol) and triethylamine (3.18  $\mu$ L, 0.0228 mmol). The reaction mixture was allowed to stir for 2 h at room temperature before it was concentrated in vacuo. Purification by column chromatography (silica, 80% EtOAc/hexanes) affords coupled product **53.1** as a colorless oil (10.0 mg, 0.0122 mmol, 74.8%, 2 steps).

To a solution of **53.1** (10.0 mg, 0.0122 mmol) in tetrahydrofuran (1.20 mL) at 0 °C was added TBAF (14.6  $\mu$ L, 1.00 M in THF) dropwise. The reaction was stirred for 2 h at 0 °C before it was diluted with ethyl ether. The organic layer was washed with 0.1 M HCl and brine solutions sequentially. The combined organic layers were dried with magnesium sulfate, filtered, and concentrated under reduced pressure. Purification by flash chromatography (silica, 100% EtOAc) provided product **1.21** in 63% (3 steps) as a clear oil.  $[\alpha]_D^{25} +18.5$  (*c* 0.6, CHCl<sub>3</sub>); <sup>1</sup>H NMR (C<sub>6</sub>D<sub>6</sub>, 400 MHz)  $\delta$  7.66 (t, *J* = 5.6 Hz, 1H), 7.24 (obs t, 1H), 6.59 (dq, *J* = 6.8, 13.6, 16.0 Hz, 1H), 5.88 (dd, *J* = 1.6, 16.0 Hz, 1H), 5.37 (dd, *J* = 0.8, 8.0 Hz, 1H), 5.27 (d, *J* = 6.0 Hz, 1H), 4.11 (q, *J* = 6.4, 12.8 Hz, 1H), 3.89 (m, 1H), 3.81 (t, *J* = 4.8 Hz, 1H), 3.72 (m, 1H), 3.58 (m, 2H), 3.42 (t, *J* = 9.4 Hz, 1H), 3.27 (m, 1H), 3.03 (t, *J* = 9.8 Hz, 1H), 2.47 (m, 3H), 2.23 (B of ABX, *J* = 10.0, 16.4 Hz, 1H), 2.00 (m, 3H), 1.85–0.85 (m, 25H), 1.65 (s, 3H), 1.43 (dd, *J* = 1.6, 6.8 Hz, 3H), 1.33 (d, *J* = 6.8 Hz, 3H), 1.26 (d, *J* = 6.4 Hz, 3H), 1.07 (d, *J* = 6.8 Hz, 3H), 0.82 (d, *J* = 6.4 Hz, 3H), 0.53 (d, *J* = 6.4 Hz, 3H); <sup>13</sup>C NMR (C<sub>6</sub>D<sub>6</sub>, 75.0 MHz)  $\delta$  197.5, 175.4, 172.7, 143.4, 138.4, 132.0, 130.5, 95.5, 80.4, 74.9, 74.2, 73.3, 72.8, 69.4, 45.9, 45.3, 43.2, 40.2, 39.5, 36.6, 36.0, 35.4, 34.7, 34.6, 34.1, 32.5, 32.3, 31.7, 31.5, 30.6, 28.5, 26.3, 22.3, 21.4, 19.8, 18.2, 17.9, 17.5, 16.0, 12.6; IR (neat)  $\nu_{\max}$  3328, 2928, 2868, 1645, 1549 cm<sup>-1</sup>; HRMS (CI, NH<sub>3</sub>) *m/z* calcd for C<sub>40</sub>H<sub>68</sub>N<sub>2</sub>NaO<sub>8</sub> [M + Na]<sup>+</sup> *m/z* calcd for 727.4873, found 727.4865.

**Acknowledgment.** Financial support for this research was obtained from NIH CA56304. J.S.P. is grateful to Amgen, Johnson & Johnson, Merck Co., Novartis, Pfizer, and GSK for financial support. I.E.W. acknowledges a Novartis Graduate Fellowship. J.T.L. acknowledges an ACS Graduate Fellowship (sponsored by Bristol-Myers Squibb) and Merck Co. Graduate Fellowship, Supported by the Intramural Research Program of the National Cancer Institute, NIH, Center for Cancer Research. Flow cytometry and cell cycle analysis were done by Kathleen Noer, Roberta Matthai, and Samantha Bauchiero of the CCR-Frederick Flow Cytometry Core, SAIC-Frederick, Inc. We thank the Developmental Therapeutics Program, NCI, for 60-cell testing. This project has been funded in part with federal funds from the National Cancer Institute, National Institutes of Health, under contract N01-CO-12400.

**Supporting Information Available:** Complete spectroscopic and analytical data including copies of <sup>1</sup>H and <sup>13</sup>C NMR spectra. This material is available free of charge via the Internet at <http://pubs.acs.org>.

JO802269Q